Large-scale flood risk assessment in data scarce areas: an application to Central Asia

Paola Ceresa[1], Gianbattista Bussi[1], Simona Denaro[1], Gabriele Coccia[1], Paolo Bazzurro[1,2], Mario Martina[1,2], Ettore Fagà[1], Carlos Avelar[3], Mario Ordaz[3], Benjamin Huerta[3], Osvaldo Garay[3], Zhanar Raimbekova[4], Kanatbek Abdrakhmatov[5], Sitora Mirzokhonova[6,9], Vakhitkhan Ismailov[7], Vladimir Belikov[8]

[1]Risk Engineering + Development (RED), Pavia, 27100, Italy
[2]Scuola Universitaria Superiore Pavia (IUSS), Pavia, 27100, Italy
[3]Evaluación de Riesgos Naturales (ERN), Mexico City, 01050, Mexico
[4]Department of Geography and Environmental Sciences, Al-Farabi Kazakh National University, A15E3C7, Al-Farabi ave., 71/19, Almaty, Kazakhstan
[5]Institute of Seismology of the National Academy of the Kyrgyz Republic, Bishkek, 720060, Kyrgyz Republic
[6]Institute of Water Problems, Hydropower Engineering and Ecology, Dushanbe, 734042, Tajikistan
[7]Institute of the Seismology of the Academy of Sciences of Uzbekistan, Tashkent, 700128, Uzbekistan
[8]Independent consultant, Ashgabat, 744000, Turkmenistan
[9]Tajik National University, Dushanbe, 734042, Tajikistan
Correspondence to: Paola Ceresa (paola.ceresa@redrisk.com)

Definizione stile: Titolo 2: Sottolineato, Inglese americano

ha eliminato: Asiaa

ha eliminato: Gabriele Coccia[1],

Abstract

The countries of Kazakhstan, Kyrgyz Republic, Tajikistan, Turkmenistan, and Uzbekistan in Central Asia are highly prone to natural hazards, particularly floods, earthquakes, and landslides. The European Union, in collaboration with the World Bank and the GFDRR, created the program "Strengthening Financial Resilience and Accelerating Risk Reduction in Central Asia" (SFRARR) to advance disaster and climate resilience in the region. As part of the SFRARR project, the "Regionally consistent risk assessment for earthquakes and floods and selective landslide scenario analysis for strengthening financial resilience and accelerating risk reduction in Central Asia" was developed to achieve the project's objectives.

A fully probabilistic risk assessment for fluvial floods has been carried out for these countries to support regional and national risk financing and insurance applications, including potential indemnity and/or parametric risk financing solutions for a regional program. A homogenized risk assessment methodology for the five countries and across multiple hazards (floods and earthquakes) and asset types has been adopted to obtain strategic financial solutions consistent across geographical areas and economic sectors.

The largest relative expected annual damages are found in Kazakhstan and Tajikistan, with values above 6‰. In the five considered countries, the largest relative expected annual damages by sector are found for the transport and agricultural sector. Climate change is expected to have contrasting impacts, with increases in risk for some regions (the most severe increase is found in Mangistauskaya Oblast in Kazakhstan) and decreases for other regions (Lebap (Turkmenistan), Khatlon (Tajikistan), Samarkand (Uzbekistan) and Batken (Kyrgyz Republic)).

This article presents the data, model, methodology and results for the five Central Asia countries of the flood risk assessment, which represents the first high-resolution regional-scale transboundary risk assessment study in the area aiming at providing tools for decision-making. The output information will inform and enable the World Bank to initiate a policy dialogue.

Keywords: flood hazard, flood risk, large-scale model, risk assessment, Central Asia

Short summary

A probabilistic flood risk assessment was carried out for five Central Asia countries for supporting regional and national risk financing and insurance applications. A homogenized risk assessment methodology for the countries and across multiple hazards (floods and earthquake) and asset types was adopted to obtain strategic financial solutions consistent across geographical areas and across economic sectors. The paper presents the first high-resolution regional-scale transboundary flood risk assessment study in the area aiming at providing tools for decision-making.

1 Introduction

Central Asia is subject to frequent disasters including earthquakes and floods (GFDRR, 2016). Furthermore, climate change, urbanization processes, and a growing population have contributed to an increase in the frequency and severity of losses caused by natural hazard events in the last two decades (Pollner et al., 2010; Yu et al., 2019; Reyer et al., 2017). The transboundary nature of many of these events requires a regional and shared approach to support, plan, and coordinate Disaster Risk Management (DRM) and Disaster Risk Financing and Insurance (DRFI) strategies. Flood risk assessment is a fundamental tool in this framework, as it allows the quantification of the expected losses caused by floods and the identification and prioritization of interventions (Tsakiris, 2014; Merz et al., 2014). Flood risk assessment is defined as an evaluation of future losses caused by floods (riverine and/or coastal) using a set of tools such as hydrological and flood models, exposure models and vulnerability models within a risk-based framework, which includes associating losses with levels of likelihood (Mitchell-Wallace et al., 2017).

In particular, large-scale risk assessment is needed by governments and international institutions to drive national-scale policies to counter economic losses by floods and improve national resilience towards disasters caused by natural hazard events. Here, we define large-scale risk assessment as a risk evaluation study that covers an area encompassing hundreds of thousands of square km, including administrative units from districts/provinces to national or pluri-national scale. Large-scale flood hazard modelling and assessment is nowadays a well-established branch of flood engineering research and practice (Alfieri et al., 2014; Pappenberger et al., 2012;

ha eliminato: The countries of Kazakhstan, Kyrgyz Republic, Tajikistan, Turkmenistan and Uzbekistan in Central Asia are highly prone to natural hazards, more specifically, floods, earthquakes, and landslides. The European Union, in collaboration with the World Bank and the GFDRR, created the program "Strengthening Financial Resilience and Accelerating Risk Reduction in Central Asia" (SFRARR), aiming to advance disaster and climate resilience in Central Asia. Within the framework of the SFRARR project, the "Regionally consistent risk assessment for earthquakes and floods and selective landslide scenario analysis for strengthening financial resilience and accelerating risk reduction in Central Asia" was conceived to help handle and achieve the parent project objectives.¶
A fully probabilistic risk assessment for pluvial and fluvial floods has been carried out for Kazakhstan, Kyrgyz Republic, Tajikistan, Turkmenistan and Uzbekistan for supporting regional and national risk financing and insurance applications, including potential indemnity and/or parametric risk financing solutions for the structuring of a regional program. The pluvial flood part of the study, however, is omitted here for brevity. A homogenized risk assessment methodology for the five countries and across multiple hazards (floods and earthquake) and asset types has been adopted to obtain strategic financial solutions consistent across geographical areas and across economic sectors.¶
This article presents the data, model, methodology and results for the five Central Asia countries of the flood risk assessment, which represents the first high-resolution regional-scale transboundary risk assessment study in the area aiming at providing tools for decision-making. The output information will inform and enable the World Bank to initiate a policy dialogue.¶

ha eliminato: Currently, the availability of risk information for Disaster Risk Management (DRM) and Disaster Risk Financing and Insurance (DRFI) activities remains variable across the region and has been provided by previous projects focusing on a single country. Moreover, few of these studies have quantified multi-hazard disaster risk, and, to our best knowledge, none have done so for the whole region using probabilistic methods applied with the sufficient fidelity required to robustly inform the development of DRFI solutions.¶

ha eliminato: ¶

Schumann et al., 2016), albeit with caveats and limitations (Bates, 2022). Large-scale flood risk modelling and assessment has also gained traction in the past years (Steinschneider et al., 2014; Ward et al., 2013) and is routinely used in commercial catastrophe risk models by insurance and reinsurance companies to price their products (Wing et al., 2020). Nevertheless, uncertainties remain large and their evaluation is subject of ongoing research (Figueiredo et al., 2018).

A key issue for large-scale model set-up and reliability is data availability. Such models are data-demanding, since they need meteorological data, river flow observations, geomorphological data, location and protection level of defences, macroeconomic data, among others. Such data might not always be available, or cannot be easily obtained, due to data restriction policies or lack of digitalisation. In Central Asia, for example, meteorological and flow data are hard to acquire without an institutional or local support. Furthermore, in this region, several flow gauges were discontinued at the time of the dissolution of the Soviet Union, and most of them were not replaced and, therefore, flow records covering recent times are scarce. Another frequent limitation is the absence of post-event survey, either of the event intensity (flood footprints) or of the physical damage and of the economic losses (e.g., damage data and insurance claims).

In this study, a flood risk assessment model was implemented based on global, regional and local datasets, which comprise a hazard module (assessment of frequency and intensity of floods), a vulnerability module (assessment of the relationship between event intensity and damage/losses) and an exposure module (inventory of building and infrastructure). The model covers the countries of Kazakhstan, Kyrgyz Republic, Tajikistan, Turkmenistan and Uzbekistan, in Central Asia. The model was implemented within the framework of the project "Regionally Consistent Risk Assessment for Earthquakes and Floods and Selective Landslide Scenario Analysis for Strengthening Financial Resilience and Accelerating Risk Reduction in Central Asia" and within the implementation of the EU-Funded "Strengthening Financial Resilience and Accelerating Risk Reduction in Central Asia" – SFRARR program (https://www.gfdrr.org/en/program/SFRARR-Central-Asia). The project aims to advance disaster and climate resilience in Central Asia countries. The landslide susceptibility assessment, which was part of this study, can be found in (Rosi et al., 2023).

The objective of this paper is twofold. First to provide guidelines for the implementation of large-scale (e.g., country-scale) flood risk models in data-scarce regions, showing that regional datasets such as reanalysis and global land maps need to be integrated with knowledge and data that can only be obtained through engagement and collaboration of local authorities and local experts through participation of stakeholders. Second to present for the five countries considered in this study the estimated levels of flood risk to support governments and decision makers in the decisions for a more comprehensive flood risk management strategy. Currently, the availability of risk information for Disaster Risk Management (DRM) and Disaster Risk Financing and Insurance (DRFI) activities remains variable across the region and has been provided by previous projects focusing on a single country. Moreover, few of these studies have quantified multi-hazard disaster risk, and, to our best knowledge, none have done so for the whole region using probabilistic methods applied with the sufficient fidelity required to robustly inform the development of DRFI solutions. Fragmented and low-resolution flood risk assessment studies already exist in the region (CAC DRMI, 2009; GFDRR, 2016; UNDP, 2014; UNISDR, 2010; Umaraliev et al., 2020; Asian Development Bank, 2015; M.S. Saidov, 2020), however a high-resolution, homogeneous, transboundary flood risk assessment such as the one presented here is unprecedented for the Central Asia region.

ha formattato: Inglese americano

2 Study area

Central Asia is highly exposed and vulnerable to a broad range of natural hazards which frequently result in economic and human losses. Flood hazard is significant in the region, with floods being the most frequent natural disaster in the period 1988-2007 according to a recent analysis provided by the Central Asia and Caucasus Disaster Risk Management Initiative (CAC DRMI, 2009). In the same period, floods were second for number of deaths caused and amount of population affected (1,512 and 19% respectively). Despite the aridity of large areas in some of the target countries, natural phenomena linked to extreme precipitation can cause billions of dollars of damages every year: collectively, floods inflict the second highest overall economic losses ($52 million), surpassed only by earthquake (an annual average of $186 million). At the local level (e.g., in Tajikistan), flood is sometimes the dominant risk in terms of economic losses (World Bank et al., 2012). Considering the deteriorated protection

infrastructure and vulnerabilities in several sectors, floods can cause considerable damage to housing, infrastructure, and agriculture (Libert, 2008).

Climatically, this region is characterized by strong rainfall gradient contrasts, due to the diversity of climate and vegetation zones. The region is drained by large, partly snow- and glacier-fed mountain rivers, that cross or terminate in arid forelands. Central Asian countries are therefore affected by a significant river flood hazard mainly in spring and summer seasons. Land use is mainly grassland in central and southern Kazakhstan, while in most of Uzbekistan and Turkmenistan vegetation is very sparse. Arable land is concentrated in northern Kazakhstan and in the irrigated parts of the plains of Uzbekistan and Turkmenistan. Tajikistan and the Kyrgyz Republic are mainly mountainous while the other three countries are mostly flat. The elevation of the region is shown in Figure 1.

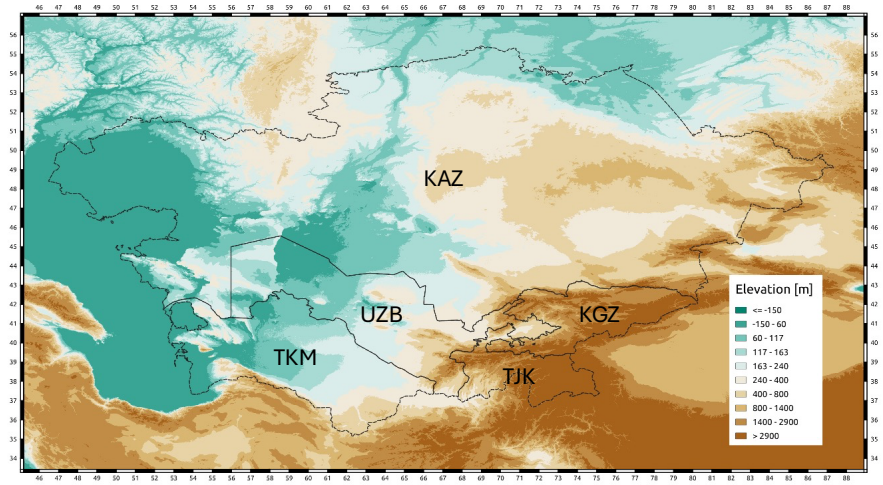

Figure 1. Study area: country boundaries and elevation.

3 Data and models

3.1 Global datasets

In this study, a wide range of well-known and established datasets was used. Table 1 shows a complete inventory of the global data and how it was used within the model. A short description of the use within the study is provided, as well as its resolution and some bibliographic references.

Table 1. Global data inventory.

Data Type	Source	Use within the model	Spatial resolution	References
Digital Elevation Model	MERIT DEM MERIT Hydro	Input to TOPKAPI, CA2D. Input to derive additional data products	3 arc-seconds	Yamazaki et al., 2017 Yamazaki et al., 2019
Soil Type	FAO Harmonized World Soil Database	TOPKAPI parametrization	30 arc-seconds	Nachtergaele et al., 2012
Land Use	GlobeLand30	TOPKAPI and CA2D parametrization.	30 m	

ha eliminato: Figure 1

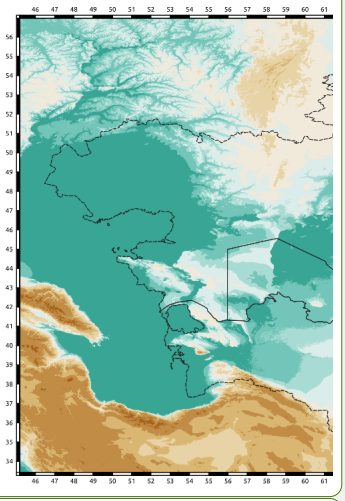

ha eliminato:

Formattato: Giustificato

ha eliminato: We utilized the ECMWF ERA5-Land (Muñoz-Sabater et al., 2021; Hersbach et al., 2019) and the KNMI Climate Explorer (Trouet and Van Oldenborgh, 2013) datasets. ERA5-Land provides hourly 0.1°×0.1° estimates for both precipitation and temperature and combines model data with observations from across the world into a globally complete and consistent dataset. ERA5 is updated daily with a latency of about 5 days. At the time of the study, the data were available from January 1981 to present but recently they were extended to cover the period from January 1951 to December 1980. We used observed data from the KNMI Climate Explorer to assess and correct the ERA5-Land extreme precipitation estimates due to the discrepancy between point station data and grid averaged data. Figure 2 shows monthly averages of rainfall in the region. ... [1]

ha eliminato: Table 1

Tabella formattata

ha formattato: Tipo di carattere: 9 pt, Inglese americano

ha eliminato: Karnieli et al., 2010

ha formattato: Tipo di carattere: 9 pt, Francese

ha formattato: Francese

ha formattato: Tipo di carattere: 9 pt, Inglese americano

ha formattato: Tipo di carattere: 9 pt, Inglese americano

Observed Discharge records	Global Runoff Data Centre (GRDC)	TOPKAPI calibration and extreme values distributions	Point measurements	
Precipitation	ERA5-Land: 1981-2020	Input to TOPKAPI simulations	0.1°	Muñoz-Sabater et al., 2021; Hersbach et al., 2019
Temperature	ERA5-Land: 1981-2020	Input to TOPKAPI	0.1°	Muñoz-Sabater et al., 2021; Hersbach et al., 2019
Reservoirs and Dams	Global Reservoir and Dam Database (GRanD)	Extreme Values Analysis and Regionalization	-	The Global Water System Project, 2011
Hydraulic defenses	FLOPROS database WorldPOP HBASE	Defended hazard maps	Administrative units 100 m 30 m	Scussolini et al., 2016 Tatem, 2017; Wang et al., 2017a
Climate change projections	CORDEX (RegCM4.3.5 driven by MPI-ESM-MR in Central Asia domain, scenario RCP4.5)	Defended hazard maps	0.2°	Giorgi et al., 2009 Ozturk et al., 2017

3.2 Local datasets

Table 2. shows a complete inventory of the data requested/obtained from the local experts and stakeholders. Although the number of available flow gauges might appear limited given the extensive region, it is crucial to recognize that their spatial distribution effectively encompasses densely populated areas where the majority of exposed assets are located. Figure 2 shows the gauging stations locations and the populated areas (in blue, population density > 1/km^2) including both local and global datasets.

Table 2. Local data inventory.

Country	Daily Discharge	Annual maximum discharge	Hydraulic Protection	Reservoirs
Kazakhstan	7 stations (records of variable lengths between 2001 and 2015)	120 stations (records of variable lengths between 1910 and 2018)	Location and length of some riverbank hydraulic structures on the Sir Darya River	Volume and year of construction of main reservoirs
Kyrgyz Republic	No data obtained because cost was too high compared to the benefit	65 stations (records of variable length between 1930 and 2018). Some of these data were purchased from KyrgyzHydroMet	Record of hydraulic protection works from 2018 at the Oblast level	Data on reservoirs' volume and construction year for 5 main reservoirs
Tajikistan	No data obtained because cost was too high compared to the benefit	14 stations (variable lengths), purchased from TajykHydroMet	No data	Volume and construction year for 13 reservoirs
Uzbekistan	2 stations (2015-2019)	46 stations (2005-2019)	No data	Volume and year of construction of main reservoirs
Turkmenistan	6 stations (2015-2020)	11 stations, variable record between 1936-2020 (monthly maxima available)	No data	Volume and year of construction of main reservoirs

ha formattato: Tipo di carattere: 9 pt, Inglese americano
ha formattato: Tipo di carattere: 9 pt, Inglese americano
ha eliminato: KNMI Climate Explorer
ha eliminato: and CA2D pluvial
ha formattato: Inglese (Regno Unito)
ha formattato: Tipo di carattere: 9 pt, Inglese americano
ha formattato: Tipo di carattere: 9 pt, Inglese americano
ha formattato: Tipo di carattere: 9 pt, Inglese americano
ha formattato: Tipo di carattere: 9 pt, Inglese americano
ha formattato: Tipo di carattere: 9 pt, Inglese americano
ha formattato: Tipo di carattere: 9 pt, Inglese americano
ha formattato: Tipo di carattere: 9 pt, Italiano
ha formattato: Tipo di carattere: 9 pt, Inglese americano
ha formattato: Italiano
ha formattato: Italiano
ha eliminato: **The impact of climate change was accounted for based on climate projections from the Coordinated Regional Climate Downscaling Experiment (CORDEX) project database *(Giorgi et al., 2009)*. In particular, the model results of the regional climate model RegCM4.3.5 driven by the MPI-ESM-MR global model in the Central Asia region (Ozturk et al., 2017), were used, under the scenario RCP4.5 (van Vuuren et al., 2011).**¶
ha eliminato: Within the SFRARR project, multiple workshops and meetings with local stakeholders and experts were held. In particular, eight capacity building workshops devoted to the different risk assessment components, namely five country-based workshops on exposure assessment and three regional thematic workshops on hazard, vulnerability and risk modelling. This activity was carried out in close collaboration with local experts and representatives from all five countries. The workshops provided participants an opportunity to learn about international best practice and latest methodologies related to natural risks assessment. These workshops allowed sharing knowledge with local experts and provided an opportunity for emergence and inclusion of a greater amount of locally collected information into the analysis.¶
Obtaining daily discharge and hydraulic protection data from local sources proved complex due to variability in data quality and form. Compiling comprehensive hydraulic protection data at the country level was hindered by its highly classified and confidential nature, posing challenges for acquisition.¶
ha eliminato: Table 2.
ha eliminato: Figure 2Figure 3
ha eliminato: and Figure 4

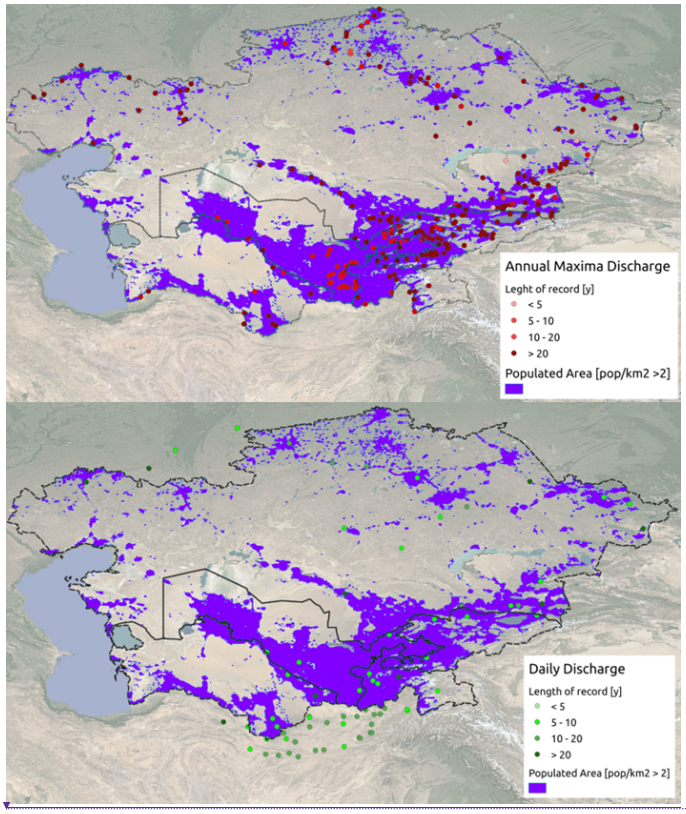

Figure 2. Annual maxima flow gauges coverage on populated areas, provided by local Institutes (top) and daily flow gauges coverage on populated areas, provided by local Institutes (inside of the country borders) and GRDC (inside and outside of the Countries' borders). . The background shades are from the MERIT DEM.

Information about the characteristics of the building stock of relevance for their vulnerability to flood water was collected from local sources and from the literature. In particular, characteristics like number of floors, presence of a basement, level of the ground floor above the street level, type of building (apartment, detached, semi-detached), etc., were collected. The number of floors distribution in various countries was derived from Pittore et al. (2020) and Wieland et al. (2015), which established floor number ranges for different building categories through local surveys. Additionally, sources such as Pittore et al. (2011) and The World Bank (2017) were used to complement the above-mentioned information. On-site collection of unit costs for building component maintenance, removal, and replacement was facilitated by local advisors and engineers, drawing from interactions with professionals involved in building design and pricing, as well as engineering manuals and real estate catalogs (such as ENiR - Uniform norms and prices for construction, installation, and repair works).

The role of the defensive protections is crucial in reducing fluvial flood hazard. However, availability of precise data regarding flood protection levels is very limited, as discussed earlier. To circumvent this problem, we developed a strategy to derive the hydraulic protection level of the region based on the correlation between the level of protection and the population density at any given location along the river. Initially, we identified urban agglomerates and determined their maximum population density through data from HBASE (Wang et al., 2017b) and WorldPop (Tatem, 2017). The former indicates the extension of urban areas, while the latter provides population density over 1 km^2. We identified the river portions afferent to each urban agglomerate by assuming

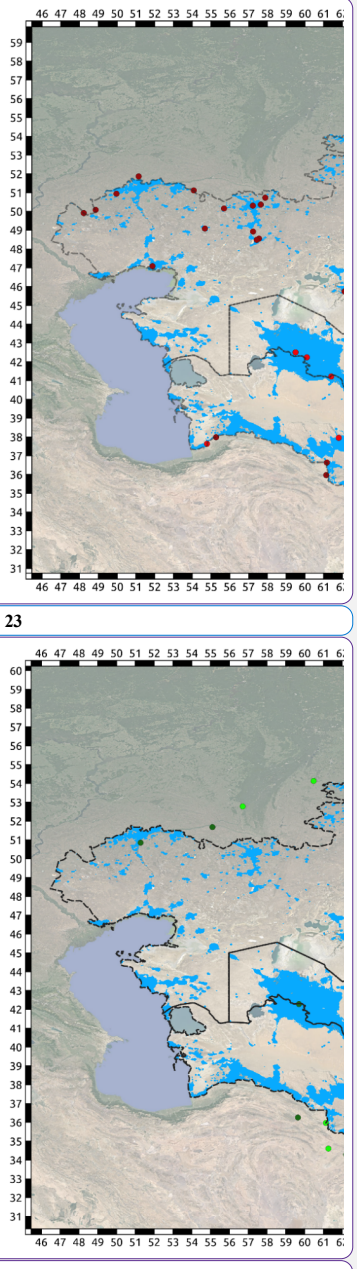

ha eliminato:

ha eliminato: 23

ha eliminato:

ha eliminato: Figure 4. Daily flow gauges coverage on populated areas, provided by local Institutes (inside of the country borders) and GRDC (inside and outside of the Countries' borders)¶

ha eliminato: These characteristics include…n particular, characteristics like number of floors, presence of a basement, level of the ground floor above the street level, type of building (apartment, detached, semi-detached), etc., were collected. The number of floors distribution in various countries was mainly …erived from (... [2]

ha eliminato: ,…(2020) and (... [3]

ha eliminato: ,…(2015), which established floor number ranges for different building categories through local surveys. Additionally, sources such as (... [4]

ha eliminato: ,…(2011) and (... [5]

ha eliminato: ,…(2017) were used to complement the above-mentioned information were consulted for the Kyrgyz Republic, while 2538 surveyed buildings in Dushanbe (Tajikistan) provided insights ... [6]

that each river reach, within a variable distance from the agglomerate whose amount depends on the accumulated area, has the same urban level of protection. Then, we associated river segments with each urban area, assuming uniform urban protection levels within variable distances from the agglomerate, determined by accumulated area size. Finally, we employed a linear scaling method using the FLOPROS database (Scussolini et al., 2016) area protection standards to refine our estimates. In specific cases, we integrated this methodology witht eh available local data. This was the case, for example, for the level of protection of the two main Kazakh cities (Almaty and Astana), for which we utilized geospatial information provided by local stakeholders.

4 Flood hazard assessment

In this study, the flood hazard of the five Central Asian countries was assessed for the historical and climate change scenario by means of a physically based numerical modelling toolset and a stochastic catalogue of flood footprints (Figure 3).

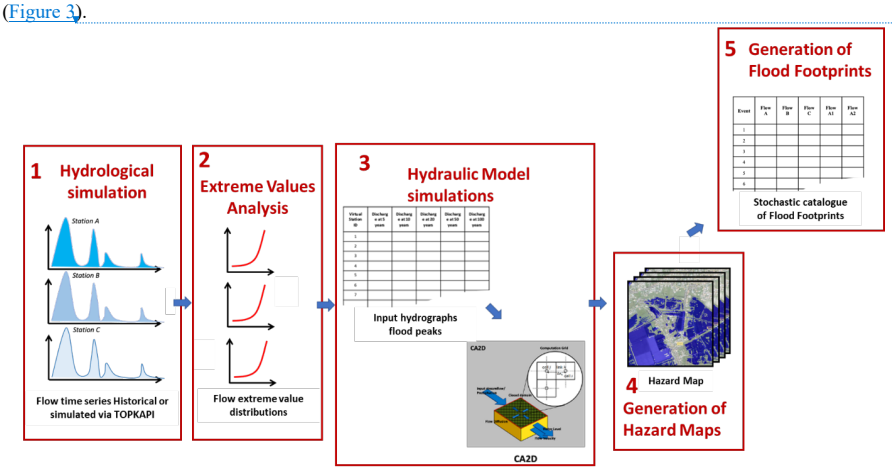

Figure 3. Flood hazard assessment: schematic representation of methodology.

4.1 Numerical Modeling Toolset

The numerical modelling toolset is composed of two elements: the hydrological model (TOPKAPI-X) and the flood hydraulic model (CA2D).

The TOPKAPI (TOPographic Kinematic APproximation and Integration) model is a fully-distributed physically-based hydrological model that can provide high resolution information on the hydrological state of a catchment (Ciarapica and Todini, 2002). The TOPKAPI-X model is an advanced version of the original TOPAKPI model that includes an additional soil layer for assessing subsurface flow, an improved snow melting and accumulation module that considers terrain aspect and latitude and a groundwater component to model the aquifer flow. The TOPKAPI-X model requires as input both precipitation and temperature meteorological data, plus a description of the soil characteristics that can be derived from the land use (to derive crop factors and surface roughness) and soil type maps (to derive soil permeability and depth).

CA2D (Dottori and Todini, 2011) is a full physically-based flood model specifically designed for high-performance computing applications, based on the cellular automata (CA) approach and the diffusive wave equations, to simulate flood inundation events involving wide areas. The model is based on the state-of-the-art of large-scale hydraulic modelling and has been tested extensively on several case studies. The CA2D model has an internal preprocessor that allows the user to provide as input only the Digital Elevation Model and the surface roughness map. The network (comprising nodes and links) is automatically generated, and specific conditions

ha eliminato: 3

ha eliminato: .3

ha eliminato: M

ha eliminato: odels

ha eliminato: As per the flood hazard assessment of the five Central Asia countries, the numerical modelling toolset is composed of two elements: the hydrological model (TOPKAPI-X) and the flood hydraulic model (CA2D).¶
The TOPKAPI (TOPographic Kinematic APproximation and Integration) model is a fully-distributed physically-based hydrological model that can provide high resolution information on the hydrological state of a catchment (Ciarapica and Todini, 2002). The TOPKAPI-X model is an advanced version of the original TOPAKPI model that includes an additional soil layer for assessing subsurface flow, an improved snow melting and accumulation module that considers terrain aspect and latitude and a groundwater component to model the aquifer flow. The TOPKAPI-X model requires as input both precipitation and temperature meteorological data, plus a description of the soil characteristics that can be derived from the land use (to derive crop factors and surface roughness) and soil type maps (to derive soil permeability and depth).¶
CA2D (Dottori and Todini, 2011) is a full physically-based flood model specifically designed for high-performance computing applications, based on the cellular automata (CA) approach and the diffusive wave equations, to simulate flood inundation events involving wide areas. A Cellular Automata (CA) is a cell-centered, finite volume scheme for the description of physical dynamic systems regulated only by local laws. In this scheme, each cell assumes a certain state (or property), which evolves in time according to specified fixed rules. In CA2D case, the momentum equation is solved for each time step, computing volume exchanges between grid cells along the cell's borders. Volumes of each cell are successively updated using flow volume conservative equations. The model is based on the state-of-the-art of large-scale hydraulic modelling and has been tested extensively on several case studies. The CA2D model has an internal preprocessor that allows the user to provide as input only the Digital Elevation Model and the surface roughness map ... [7]

ha eliminato: Flood vulnerability for buildings was assessed using a component-based flood vulnerability model, called INSYDE (Dottori et al., 2016). This model account for different measures of the event intensity (water depth, but also flow velocity, flood duration, sediment load, water ... [8]

ha eliminato: 43.1 Flood hazard assessment¶

ha eliminato: Figure 3Figure 5

ha eliminato: 35

ha eliminato: The modelling steps followed in this study were:¶
ERA5-Land hourly precipitation and temperature on a 0.1×0.1° regular grid were processed and used to drive calibrated TOPKAPI-X set-ups (one for each catchm ... [9]

ha eliminato: A stochastic catalogue of events was generated by assessing the historical correlation among flows of all the river reaches and extracting randomly reach-specific footprints from the hazard maps according to the cross-correlation derived from historical flow series.¶

Formattato: Normale, SpazioDopo: 0 pt, Nessun elenco puntato o numerato

(such as flood protections) can be included, where present. In addition, input meteorological data must be provided in the form of hydrographs at specific points and/or of rainfall maps. We ran the model using the semi-inertial formulation of the momentum equation, which was developed for the LISFLOOD-FP model (Bates et al., 2010). This approach allows for high resolution simulations at a significantly reduced computational effort, making it possible to run hydraulic simulations at the continental and global scale (Dottori and Todini, 2011).

4.1.1 Hydrological model

ERA5-Land hourly precipitation and temperature on a 0.1×0.1° regular grid were processed and used to drive calibrated TOPKAPI-X set-ups (one for each catchment in the region, including catchments partially overlaying neighbouring countries such as China, Afghanistan and Russia). The output was a set of 40-years long hourly discharge values at numerous river sections covering the whole drainage network in the region.

The TOPKAPI-X model was run on a regular 1×1 km grid for all catchments in the region, based on a resampled digital elevation model consistent with MERIT-Hydro in terms of flow direction and river network. The hydrological model uses an equal-area projected reference system. Rainfall and temperature values, which are defined on a regular 0.1° grid with geographical coordinates, were associated to each of the hydrological model grid using a simple nearest neighbour methodology. Soil type and land use maps were also resampled to match the same grid. The model was run on an hourly time-step using hourly ERA5-Land precipitation and temperature from January 1981 to December 2020. The model simulations were initiated with average soil saturation and river depth conditions and the first year of simulation was used as warm-up period to reach realistic soil moisture conditions. Therefore, the year 1981 was not considered for calibration purposes nor for the extreme value analysis. The main model output consisted of hourly simulated discharges at several locations of the river network across the entire region. The model simulations corresponding to locations where observations were available have been used to perform a trial-and-error calibration that could reasonably reproduce the overall behaviour of each catchment.

The TOPKAPI-X model was calibrated through a trial-and-error procedure adapting the initial model parameters in order to match the available observed discharge. We mainly based the model calibration on the historical daily data, but also used the annual maxima for the areas where daily data were not available. The calibration process focused mainly on robustly reproducing the flow peaks. This is because the hydrological simulations aim at estimating the extreme discharge value distributions at river sections across the region that are used to derive the flood footprint at different return periods via the hydraulic model. Since a physically based model better reproduces the flow peaks if all the other hydrological components are well represented, we made sure that the main hydrological processes were also correctly reproduced, with particular attention to the snow accumulation/melting component, which is the driver of most of the floods in this region. The calibration was performed independently for each catchment where historical data were available. Given the distributed and physically based nature of the TOPKAPI-X hydrological model, the calibration process was not based on an automatic procedure but on the use of reasonable values of the physical parameters. This procedure allows the identification of model parameters values that provide reasonable outputs across the entire catchments, avoiding under- or over-fitting any of the available historical records. We assumed two soil layers (superficial and sub-superficial) and the parameters that were calibrated included horizontal conductivity and depth for each of the two layers, vertical conductivity, potential evapotranspiration and snowmelt rate. The calibration period varied among historical stations, with record lengths ranging from 15 to 37 years.

4.1.2 Extreme value analysis

For each river section, an extreme value analysis was carried out by fitting a Generalised Extreme Value distribution (Jenkinson, 1955) over the 40 annual maxima derived with TOPKAPI-X. Given the shortness of this series, the uncertainties in the input data and the alterations to flow regime caused by lakes and dams, a correction procedure was established to incorporate flow records, where available. This procedure corrects the resulting extreme value distributions with the objective of maximising the similarity between observed and modelled extreme flows. The output of this step is composed of several discharge values at fixed exceedance probabilities (1-in-5, 10, 20, 50, 100, 200, 500, 1000 years floods) for each river section.

ha eliminato: **More information about these five steps is provided below.**¶

ha eliminato: **3**

ha eliminato: has been

ha eliminato: During the extreme value analysis calibration process, the main limitations of the hydrological model application were considered:¶
Absence of lake/reservoirs modeling. The influence of lakes and reservoirs was taken into account by allowing an overestimation of the flood peaks and underestimation of the low flows for for downstream stations of primary reservoirs. These reservoirs effectively attenuate flood waves by storing water during peak events and releasing it during drier periods. This behavior was not explicitly modeled due to lack of information on the reservoir management strategies. Hence, it was anticipated that the model would not precisely replicate observed hydrographs for stations located downstream of reservoirs (e.g., the Turkmenabat, Kerki (former Atamurat), Semiyarskoje and Chirchik stations in Figure 7).¶
Inability to reproduce the effect of alluvial plains, which similarly to reservoirs alter flood waves by flattening peak flows. To address this, the same approach was adopted as with reservoirs, namely we allowed the overestimation of the peaks and the underestimation of recession curves (e.g, evident at stations like the Kushum and Gram in Figure 7) for stations located within alluvial plains.

ha eliminato: ¶

ha formattato: Inglese americano

ha eliminato: **3**

ha eliminato: ¶

The extreme value analysis and regionalisation process was based on fitting the Generalized Extreme Value (GEV) distribution for several locations along the drainage network to derive the peak flows with different return periods. GEV is a standard tool for modeling flood peaks using annual maximum series (Morrison and Smith, 2002; Rosbjerg and Madsen, 1995). Simulated flow annual maxima were used to derive a GEV distribution for a large number of river sections all over the river network. Where observed flow records were available, the GEV distribution was also fitted on the observed flow annual maxima, and the resulting distribution compared with the distribution derived from simulated flow values with the objective of evaluating the model error on the extreme values. We observed that the largest hydrological model discrepancies occur on the main stem of large rivers, because of the impact of large reservoirs and floodplains. Therefore, an adjustment of the simulated flows was implemented by computing the ratio between observed and simulated mean annual maximum flows and then multiplying the simulated flow by such a ratio. In other terms, the simulated annual maximum flows were increased or decreased by a coefficient based on the mean bias between observed and simulated mean annual maximum flows. Where observed data were not available, the adjustment coefficient was computed by using an adjustment coefficient from an associated station selected based on the proximity of the location and flow accumulated area. This procedure yielded a very good fit between observed and simulated extreme values of flow and allowed extrapolating the adjustment to ungauged river sections. This adjustment was particularly useful in floodplains and downstream dams, which are features that are particularly difficult to reproduce with a hydrological model. With this procedure we obtained estimates of the extreme flow value distribution for 78,000 river sections having more than 100 km^2 drainage area, from which peak flows were extracted at several levels of likelihood (1-in-5, 10, 20, 50, 100, 200, 500, 1000 years).

4.1.3 Hydraulic model

At each river section, the CA2D model was used to simulate the flood propagation of the river discharges generated at step 2), producing reach-specific water depth footprints for each of the fixed exceedance probability levels.

The CA2D model was run at a 3 arcseconds (~90 m) spatial resolution. The simulation time-step is dynamic, and it varies between 0.01 and 15 seconds, with the maximum allowable time step defined by the Courant–Friedrichs–Lewy or CFL condition (Courant et al., 1928), which is commonly adopted to preserve stability in computational fluid dynamics models. For every one of the 78,000 river reaches, 8 simulations were carried out using the 1-in-5, 10, 20, 50, 100, 200, 500 and 1000 flows resulting from the extreme value analysis as boundary conditions. The MERIT-Hydro model was used as a source of elevation data and GlobeLand30 was used to derive roughness values from land use classes (Arcement, et al., 1989). The calibration of the CA2D model primarily focused on reproducing historical event hydrographs in terms of volume and peak timing: for each river section, we built a flood hydrograph to estimate the time of concentration, i.e., the time needed for the water to flow from the most remote point in a watershed to the watershed outlet (Giandotti, 1934). We assumed a triangular hydrograph reaching the flood peak at 2/3 of the concentration time and going back to zero at twice the concentration time. We assume the bankfull discharge as the discharge at 2-year return period.

Flood protections were not explicitly accounted for in CA2D simulations. Instead, we adjusted water depth maps to reflect the presence of flood protections. Specifically, we assumed that areas with water depths below the designated level of protection would not incur any losses.

4.1.4 Flood extent map validation

For a single flood event, occurred in Hamadoni, Tajikistan, in 2005, reported losses, flood footprints, and river flow time series were available (Saidov et al., 2006, JICA, 2007). The availability of such data allowed for the validation of some of the components of the present model (namely the hydraulic model and the risk model), although limited to only one event. Nevertheless, and despite the caveats of carrying out a validation of a model against a single observation, showing the performances of the risk model for such event has an informative value.

In order to validate the hydraulic model, the observed flood extent as well as the inlet discharge data were extracted from the JICA report (JICA, 2007).

ha eliminato: 3

ha eliminato: Flood h

ha eliminato: 0.00083°

ha eliminato: F

ha eliminato: The role of the defensive protections is crucial in reducing fluvial flood hazard. However, availability of precise data regarding flood protection levels is very limited, as discussed earlier. To circumvent this problem, we developed a strategy to derive the hydraulic protection level of the region based on the correlation between the level of protection and the population density at any given location along the river. Initially, we identified urban agglomerates and determined their maximum population density through data from HBASE (Wang et al., 2017b) and WorldPop (Tatem, 2017). The former indicates the extension of urban areas, while the latter provides population density over 1 km^2. We identified the river portions afferent to each urban agglomerate by assuming that each river reach, within a variable distance from the agglomerate whose amount depends on the accumulated area, has the same urban level of protection. Then, we associated river segments with each urban area, assuming uniform urban protection levels within variable distances from the agglomerate, determined by accumulated area size. Finally, we employed a linear scaling method using the FLOPROS database (Scussolini et al., 2016) area protection standards to refine our estimates.The estimated correlation was then linearly scaled using the area protection standards provided by the FLOPROS database (Scussolini et al., 2016). To apply this strategy, we first identified urban agglomerates and calculated the corresponding maximum population density using the HBASE (Wang et al., 2017b) and WorldPop (Tatem, 2017) datasets. The former indicates the extension of urban areas, while the latter provides population density over 1 km^2. We identified the river portions afferent to each urban agglomerate by assuming that each river reach, within a variable distance from the agglomerate whose amount depends on the accumulated area, has the same urban level of protection. Finally, we assigned a level of protection to each river tract afferent to the agglomerate, based on the relationship previously estimated with the population density and the area's FLOPROS protection standards. When possible, we integrated into these estimates the localized and mainly qualitative data obtained from the local partners. This was the case, for example, for the level of protection of the two main Kazakh cities (Almaty and Astana), for which we utilized geospatial information provided by local stakeholders.…

ha formattato: Inglese americano

ha formattato: Tipo di carattere: Non Grassetto

ha formattato: Tipo di carattere: Non Grassetto

The flood event was quite long and involved a dyke breach and extensive damage to the nearby villages. The JICA study provides both a probable inundation area that was estimated from satellite data, and a flood footprint that was simulated.

The following factors contribute to the uncertainty in both the JICA results and ours:

- Satellite data from SPOT and ASTER are only available before and significantly after the peak. This probably explains the satellite estimated flood map underestimation of the flood extent.
- The inlet discharge was estimated from the data recorded at a different station which is located at 80 km upstream, by the peak discharge ratio.
- The simulated water depth values are not available from the JICA study, we only have a figure that we superimposed over our flood footprint for a visual comparison.
- We did not simulate the dyke breach as information on its location and the nature of the damage was not available.

We built our hydrograph by taking the data estimated by JICA and used it as input to the CA2D model to get the flood footprint for the event. Figure 4 compares the CA2D simulated flood map (in yellow) with the satellite-estimated flood map (left) and the JICA study's simulated flood map (right).

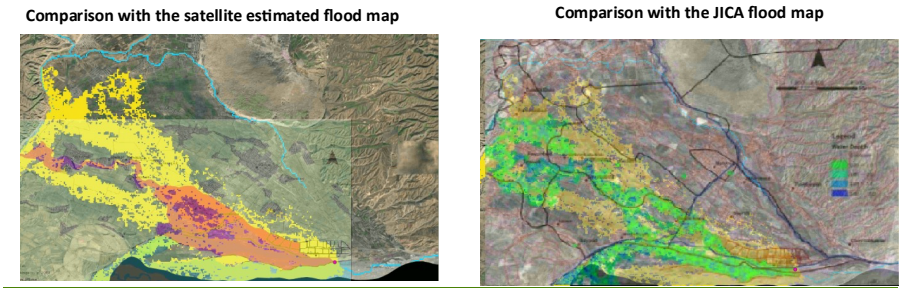

Figure 4. Flood extent maps comparison

4.2 Stocasthic catalogue of flood footprints

The results of the flood model simulations were the hazard maps, i.e., water depth maps at fixed return periods. While hazard maps provide the depth of inundation that can occur at a given location with a certain annual probability (or, conversely, with a certain return period), they are unable to describe the likelihood of concurrent flooding across multiple sites. This caveat limits their capability of assessing risk over the full range of plausible scenarios, including the most extreme ones which are those of most concerns to stakeholders. For this purpose, risk assessment models routinely use stochastic catalogues of events, i.e., datasets of synthetic event intensity footprints. This procedure is typically used for rainfall events (Salazar et al., 2009; Francés et al., 2011), tropical cyclones (Bloemendaal et al., 2020), drought (Guillod et al., 2018) and other perils. In this study, a flood depth hazard catalogue serves this purpose, by providing a stochastic ensemble of 10,000 years of hypothetical floods that may occur in the region, with related annual frequency of occurrence. To ensure spatial coherence in the stochastic catalogue, the spatial correlation of the river flow at each gauge/station is determined by computing a cross correlation matrix based on all the available (observed/simulated) flow time series. The methodology followed to produce a stochastic catalogue consists of the following steps:

1. Clustering: river sections are grouped into clusters under the assumption that flows at river sections in the same cluster are highly correlated random variables. The amount of correlation depends on historical simulated flows, location of the stations and accumulated areas of the stations.
2. Cluster activation probability: the annual probability of activation of a cluster is computed, where "activation" is defined here as an instance when at least one river section in a given cluster exceeds the 5-year flow. This probability is based on the activation of clusters in the historical simulated flows.

ha formattato: Tipo di carattere: Non Grassetto
ha formattato: Tipo di carattere: Non Grassetto
ha formattato: Tipo di carattere: Non Grassetto
ha formattato: Tipo di carattere: Non Grassetto
ha formattato: Tipo di carattere: Non Grassetto
ha formattato: Tipo di carattere: Non Grassetto
Formattato: Paragrafo elenco;References;Main numbered paragraph;List Paragraph (numbered (a));Normal 2;List_Paragraph;Multilevel para_II;List Paragraph1;Numbered List Paragraph;Bullets;Colorful List - Accent 11;123 List Paragraph;Body;Bullet;Normal 2 DC;Liste 1, Puntato + Livello:1 + Allinea a: 0.63 cm + Imposta un rientro di: 1.27 cm
ha eliminato: Figure 3
ha eliminato: 3
ha formattato: Tipo di carattere: Non Grassetto
ha eliminato: 3
ha eliminato: 1.4
ha eliminato: Hazard maps
ha eliminato: ¶
ha formattato: Tipo di carattere: Grassetto, Sottolineato, Inglese americano
Codice campo modificato

3. Activation of river section within a cluster: the average number of active river sections for a given year and its standard deviation are computed. A station is defined to be active when the flow at that location exceeds the 5-year flow. These values are based on the activation of clusters in the historical simulated flows.
4. Generation of the stochastic catalogue: based on all the analysis above (clusters, annual activation probability, average number of active stations) and on the hazard curves at each section, a stochastic catalogue is produced, with equivalent duration of 10,000 years. Every year consists of an annual flood footprint, i.e., a map where each pixel represents the maximum water depth during a given year.

4.3 Climate change scenario

The climate scenarios used in this study are detailed in Ozturk et al. (2017). The Regional Climate Model (RCM) RegCM4.3.5 from the International Centre for Theoretical Physics (ICTP) was driven by two different CMIP5 Global Climate Models (GCMs): the HadGEM2-ES from the UK Met Office Hadley Centre and the MPI-ESM-MR from the German Max Planck Institute for Meteorology, under two emission scenarios (RCP4.5 and RCP8.5). Based on predictive performance, we selected the MPI-ESM-MR GCM. We chose RCP4.5 over RCP8.5 because it aligns more closely with current emission trends and future reduction pledges (Roger Pielke Jr et al., 2022). The model was run over the Central Asia domain as defined by CORDEX (Giorgi et al., 2009), with the corner points at 54.76°N - 11.05°E, 56.48°N - 139.13°E, 18.34°N - 42.41°E, and 19.39°N - 108.44°E.

The impact of climate change on flood hazard was accounted for by estimating change factors to the ERA5-Land precipitation and temperature based on the probability density function (pdf) comparison of the current climate and 1971-2100 projection. Bias-correcting climate projections before using them in hydrological modelling is standard practice and should always be carried out to avoid propagating the climate model biases into the hydrological model results (Shrestha et al., 2017; Teutschbein and Seibert, 2012). The methodology we used here belongs to the "delta change" family cited by Teutschbein and Seibert (2012). The literature on this methodology and its implications on hydrological model outputs is very extensive and well documented, here we cite only a few examples (Räty et al., 2014, 2018; Mudbhatkal and Mahesha, 2018; Fang et al., 2015). It is simpler than other techniques, since it does not require to bias-correct the baseline climatology (which is still the observed climatology), although it has the disadvantage that some properties of the variable to be corrected still remain unadjusted (for example, if the precipitation from a certain climate projection is simply multiplied by a factor in order to reproduce the annual average of the reference dataset, the distribution of the original reference dataset will be maintained and only the mean values will be corrected – this is also called "constant scaling"). However, the approach used in this paper, which adjust the whole distribution of precipitation and temperature, not only the mean or the standard deviation, limits this disadvantage. Räty et al. (2014), among others, have discussed the advantage and disadvantages of such technique, which blends the simplicity of the delta factor methodologies with the robustness of the quantile mapping methodologies. We used a probability density function matching technique to modify the distributions of the current ERA5-Land variables (Lafon et al., 2013).

To derive the hazard maps for the time horizon 2080 (i.e., the time window 2071-2100), the entire modeling chain composed of hydrological modeling (TOPKAPI-X), extreme values analysis and hydraulic modeling (CA2D) was fed with the modified ERA5-Land derived meteorological input data (precipitation and temperature). Although we are fully cognizant that flood hazard and risk estimates under scenarios of climate change are affected by a very large uncertainty (Bubeck et al., 2011), it is of paramount importance that the effects of climate change be considered into any disaster risk management strategy to ensure robust planning going forward.

5 Flood risk assessment

5.1 Vulnerability and exposure

Flood vulnerability for buildings was assessed using a component-based flood vulnerability model, called INSYDE (Dottori et al., 2016). This model account for different measures of the event intensity (water depth, but also flow velocity, flood duration, sediment load, water quality, etc.) and different components of the building (structural, non-structural, finishing, doors/windows, systems, basement, etc.) to derive a large set of curves for

ha eliminato: 3
ha eliminato: 1.5
ha eliminato: ¶
Formattato: Titolo 2
ha eliminato: (
ha eliminato: ,
ha eliminato: (
ha eliminato: ,
ha eliminato: 4
ha eliminato: .2
ha eliminato: 4

each component of the damage. These curves are then combined depending on the characteristics of the building categories. Local knowledge was key in the construction of vulnerability curves for buildings, in terms of defining unit costs of the components, archetype buildings, materials, etc.

INSYDE is a very flexible vulnerability model, suitable for both data-rich and data-poor scenarios. In this study, a specific vulnerability function relating water depth and level of damage was set up for each of the taxonomy categories: Residential (unreinforced masonry, unreinforced masonry concrete floors, confined masonry, reinforced masonry, low rise, reinforced masonry, medium rise, reinforced concrete frame without earthquake-resistant design, reinforced concrete frame with moderate earthquake-resistant design, reinforced concrete frame with high level of earthquake-resistant design, reinforced concrete walls without earthquake-resistant design, reinforced concrete walls with moderate level of earthquake-resistant design, reinforced concrete walls with high level of earthquake-resistant design, adobe, timber structure, timber structure, steel structure, other structure, schools, hospitals, commercial, industrial (Scaini et al., 2024a, b)). Note that the categorisation is, in some cases, done based on criteria that are not relevant to flood risk (e.g., earthquake-resistant design does not affect flood damage). This was done in order to ensure compatibility with a companion earthquake risk model.

Some flood-relevant parameters were not explicitly considered in the categorisation, due to lack of spatialised data, for example the presence of a basement, the number of storeys or the height of the ground level over the surrounding terrain. These parameters were treated in a statistical way. For example, if, within a certain category, the percentage of buildings with one storey is 40% and the percentage of buildings with two storeys is 60%, the final vulnerability curve was obtained as the weighted average of two curves, one considering a one-storey building, the other considering a two-storey building. The distributions of such parameters were obtained from the available literature (Pittore et al., 2011, 2020; The World Bank, 2017; Wieland et al., 2015), from local institutions (for example, the Kazakh Research and Design Institute of Construction and Architecture – KazNIISA), from local surveys (for example, in Dushanbe, Tajikistan, from Pittore et al., 2020) and from polls and consultations with local experts carried out during several workshops in 2021 an 2022 and organised by the World Bank.

The component-based approach also requires unit costs for each component. These are the costs per unit (usually per m, m^2 or m^3) of cleaning/removing/replacing each of the component. These costs have been collected onsite by local advisors and engineers through inquiries with engineers and architects involved in the design and pricing of buildings and from engineering manuals or real estate catalogues (for example, the ENiR - Uniform norms and prices for construction, installation and repairing works).

Local knowledge was key in the construction of vulnerability curves for buildings, in terms of defining unit costs of the components, archetype buildings, materials, etc. This knowledge, together with the literature cited above and the collaboration with local institutions and experts led to produce vulnerability curves that are highly suitable for the local context, as opposed to the common practice of transferring curves developed elsewhere without considering the local context. This approach also allowed producing separate curves for each country.

The infrastructure vulnerability (e.g., roads, power plants, airports) was taken from the Global Flood Depth-Damage dataset developed by the European Union's Joint Research Centre (Dottori et al., 2018; Huizinga et al., 2017) and from HAZUS (HAZard United States) (FEMA, 2018), the natural hazard analysis tool developed and freely distributed by the US Federal Emergency Management Agency (FEMA).

Flood vulnerability for the two prevalent crops, cotton and wheat, were derived from the literature. The cotton curve was derived from Qian et al. (2020). The wheat curve was derived from similar crops (no specific wheat curves were found for Central Asia, or Asia in general, but vulnerability curves for other cereals in Asia exist) (Baky et al., 2020; Hendrawan and Komori, 2021; Kwak et al., 2015; Molinari et al., 2019; Win et al., 2018).

An exposure database for the region (Scaini et al., 2024a, b), which includes residential and non-residential buildings, transportation infrastructure and crops, was developed by assembling available global and regional datasets with country-based information provided by local authorities and research groups, including reconstruction costs. We refer to the original paper for more information.

Although this article discusses only the flood-induced losses, as alluded to before this effort was part of a multi-hazard risk assessment study that included also assessing risk for earthquakes (for the earthquake risk assessment please refer to Salgado et al. (2023). To compare the risk across different perils, it was necessary to use a peril-agnostic assessment methodology such as that adopted in CAPRA, which uses a common representation of the disaster risk assessment components, i.e., hazard, exposure, and vulnerability. Since the simultaneous occurrence

ha eliminato: (
ha eliminato:)
ha formattato: Apice
ha formattato: Apice
ha eliminato: (
ha eliminato: ,
ha formattato: Inglese (Regno Unito)

of earthquakes and floods (at least of those causing the large losses of interest to stakeholders) is highly unlikely, the losses caused by the two types of events have been assumed to be independent. The CAPRA platform (www.ecapra.org) is an open-source and free platform for multi-hazard probabilistic and deterministic risk assessment, that has been developed with the initial financial support of the World Bank, the Inter-American Development Bank and the UNISDR (Reinoso et al., 2018). The CAPRA Platform, which allows multi-peril assessment (using the probabilistic methodologies described in this manuscript) uses the geographical information (for the exposure and hazard components) and produces economic losses aligned with the risk metrics typically employed in the insurance industry, besides. Moreover, it produces GIS-compatible geospatial data layers with metadata, describing estimated loss per administrative unit, as well as identifying the location of key industrial sites, critical and supply infrastructure and the corresponding hazard intensity values at those locations, either in raster or vector formats.

5.2 Risk assessment

The flood risk of the five Central Asian countries was assessed by means of the CAPRA risk assessment software (Reinoso et al., 2018) according to the methodology displayed in Figure 5.

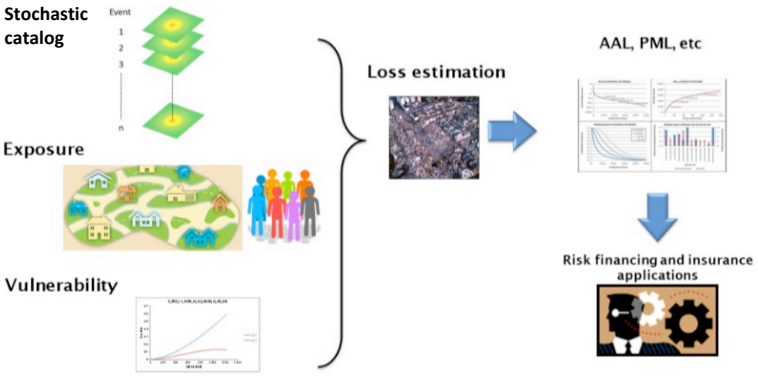

Figure 5. Flood risk assessment: schematic representation of methodology.

The loss estimation module allows estimating both the economic losses for the assets in the exposure datasets and corresponding human losses for each of the possible future events in the stochastic catalogue. Economic losses for each exposed asset are determined by combining the flood depth distribution at the site with the corresponding damage function. This yields a distribution of mean damage ratios (repair cost divided by asset replacement cost) for each asset. Scaling this distribution by the total asset value generates the loss distribution caused by a flood event. Summing these losses for all exposed assets provides the total loss for the event.

The flood risk model presented here is designed to provide all the loss metrics needed to devise risk mitigation strategies, including the design of an insurance product. Key outcomes of the long-term flood risk assessment are the year loss tables (YLTs) for each of the five analyzed countries. These YLTs detail the expected value and the corresponding uncertainty of the economic loss, together with its annual frequency of occurrence, and a timestamp (ranging from year 1 to year 10,000) for each event in the stochastic set. The YLTs can then be used to derive the loss exceedance curve (LEC), also known as the Exceedance Probability (EP) curve (e.g., Mitchell-Wallace et al., 2017), which encapsulates loss occurrence characteristics and informs disaster risk management activities, such as regional and national risk financing and insurance development. Additionally, the model yields estimate of key risk measures like average annual loss (AAL) and probable maximum loss (PML), commonly used for risk communication.

5.3 Risk model calibration

Although all the components of the risk assessment developed in the project (hazard, exposure, and vulnerability) have been separately validated against observations to the extent possible, it is good practice to calibrate and

ha eliminato: 4
ha eliminato: ¶
Formattato: Normale
ha eliminato: As stated earlier, t
ha eliminato: Figure 4Figure 6
ha eliminato: 46
ha eliminato: The flood risk model introduced is designed to furnish necessary loss metrics for formulating risk reduction strategies, including insurance product design. Key outcomes of the long-term flood risk assessment are the year loss tables (YLTs) for each of the five analyzed countries. These YLTs detail economic loss expectations, uncertainty, annual occurrence frequency, and a timestamp (ranging from year 1 to year 10,000) for each event in the stochastic set. Using this simulated data, one can estimate either the aggregate yearly occurrence probability of losses exceeding a threshold or the annual probability of the maximum event loss surpassing a threshold. The YLTs enable the derivation of a loss exceedance curve (LEC), which encapsulates loss occurrence characteristics and informs disaster risk management activities, such as regional and national risk financing and insurance development. Additionally, the model yields estimate of key risk measures like average annual loss (AAL) and probable maximum loss (PML), commonly used for risk communication.¶
ha eliminato: 4
Formattato: Titolo 2

validate the risk model as a whole. This further calibration step, when needed, often adjusts the exposure and vulnerability module to ensure a better agreement among historical observations of economic losses and modelled losses.

Risk model calibration and validation are typically carried out by comparing modelled and observed loss estimates for historical events, adjusting some of the model parameters or components to improve the goodness-of-fit. Observed loss estimates are usually obtained from post-event assessment reports and surveys. However, limited and uncertain historical flood loss data in Central Asia hinder this calibration. This scarcity of loss data limits the efficacy of the flood risk model calibration effort.

Given the data limitation, it was decided to reduce the number of calibration parameters to a minimum. Hence, all the vulnerability curves were increased or decreased by the same amount, i.e., no differential calibration was carried out on vulnerability curves of different exposure classes or different countries. Furthermore, only the residential building vulnerability curves were calibrated, since residential buildings account for the majority of the exposed value. Infrastructure and crop vulnerability functions were left unadjusted, as no data were available to justify a specific calibration of such curves. Bearing in mind these data availability limitations and the objective of the present risk assessment (which is to estimate the underlying, long-term average flood risk), the model calibration was carried out as follows:

1. A list of historical events and reported losses was collected from local governments/agencies within the project;
2. The districts/regions affected by the historical floods were identified;
3. The risk model was run using the stochastic catalog of flood footprints as input, for all the district/regions previously identified;
4. The exceedance probability curves of all selected district/regions were calculated based on the results of the simulations with the stochastic catalogue;
5. Based on the resulting exceedance probability curves, the return periods of the historical losses were computed (historical losses and district/region losses are comparable under the assumption that reported events are usually large floods that either affect the whole district/region or represent economic losses that are significant at the scale of the whole district/region);
6. The resulting return periods were critically analyzed under the following assumptions:
    a. Reported events are typically large events that make the news, and therefore are relatively rare. It is expected that their return period is at least 5 years.
    b. It is relatively unlikely that a reported flood event has a return period of more than 500-1,000 years.
    c. If a region has more than one reported event, it is highly unlikely that all events have return periods longer than 100 years.
    d. In general, it is expected that most reported floods have a return period between 5 and 100 years, with very few outliers.
7. If some of the above criteria were not met, the vulnerability curves were adjusted to increase or decrease the losses and obtain a better adjustment to the criteria.

The reported monetary and human losses were collected from a variety of sources, including EM-DAT (EM-DAT CRED, 2010), AON's catastrophe insight reports, SwissRe's Sigma explorer, and, in some cases, from local sources. The international databases already provide loss figures in USD dollars. Conversion from local currency to USD for data collected from local sources was done using the average currency exchange rate of the year the disaster happened. Loss values were then trended to account for inflation and growth since the moment of occurrence of the flood, using real GDP growth as a proxy. Although affected by large uncertainties, these are the only datasets available for model calibration, as presented below.

The rational of this methodology is that, instead of providing direct comparisons between observed and reported losses (not possible given the lack of available data), the calibration process tries to demonstrate that the model is providing risk estimates that are in line with what has been observed in the past 20 years in terms of frequency of the events and severity of the economic losses. Given the objective and the limitations described above, this seems to be the most tenable strategy that both exploits the, albeit rare, data available and provides sensible loss estimates.

Human vulnerability curves were calibrated based on national-scale statistics of fatalities caused by floods. Vulnerability functions were adjusted so that the average number of fatalities per year provided by the model was similar to the values obtained from the official statistics.

ha eliminato: Given the data limitation, it was decided to reduce the number of calibration parameters to a minimum. Hence, all the vulnerability curves were increased or decreased by the same amount, i.e., no differential calibration was carried out on vulnerability curves of different exposure classes or different countries. Furthermore, only the residential building vulnerability curves were calibrated, since residential buildings account for the majority of the exposed value. Infrastructure and crop vulnerability functions were left unadjusted, as no data were available to justify a specific calibration of such curves.¶

ha eliminato: , especially as detailed flood depth maps are rare. Such maps enable the reduction of the uncertainty in the estimation the water depth estimates, so that any discrepancy between observed and modelled losses can be more clearly attributed to the vulnerability or the exposure components of the risk model. In Central Asia unfortunately only one historical flood event has these characteristics (flood depth map and post-event loss assessment), namely the 2005 Hamadoni flood in Tajikistan (Saidov et al., 2006).

ha eliminato: ¶

ha formattato: Inglese (Regno Unito)

5.4 Risk model validation:

5.4.1 Exceedance Probability (EP) loss curves

We compared the EP loss curves for those Oblasts where partial historical loss data were available (). This procedure consisted of verifying that the reported losses for 8 historical floods were coherent with the results, by Oblast, in terms of the EP curves (i.e., reviewing that there were no systematic under- or over-estimation of losses). shows one of the results of these comparisons.

Table 3. Reported economic losses for flood events and identification of the oblast where it occurred.

Event	Country	Oblast	Reported loss (US M)
Flood_TJK_2010-5-6	Tajikistan	Khatlon	$307.30
Flood_TJK_2006-4-21	Tajikistan	Khatlon	$264.68
Flood_TJK_2005-7-23	Tajikistan	Khatlon	$156.06
Flood_TJK_2021-5-7	Tajikistan	Khatlon	$8.40
Flood_TJK_2014-4-22	Tajikistan	Khatlon	$3.04
Flood_KAZ_2010-2-	Kazakhstan	Almaty	$73.44
Flood_KGZ_2012-4-23	Kyrgyzstan	Osh & Batken	$24.42
Flood_KGZ_2005-6-10	Kyrgyzstan	Osh & Batken	$8.03

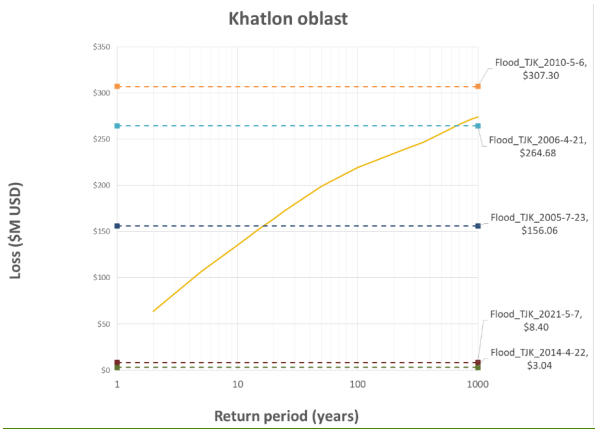

Figure 6. EP curve and reported economic losses for the Khatlon Oblast in Tajikistan

5.4.2 The Hamadoni 2005 flood event

Losses for the Hamadoni event are estimated to be in the order of 7 to 10 M USD (Saidov et al., 2006). The model presented in this paper estimated losses of 10 M USD, which shows a very good agreement between modelled and reported losses. However, the present model has been set up considering 2022 prices and exposure, while the reported losses refer to 2005 prices and exposure, and therefore this value must be corrected to account for such factors. A simple way to do this is to account for price inflation and changes in exposure using Gross Domestic Product (GDP) as a proxy. Changes in GDP in time are indeed a measure of the changes of the economy of a country. According to the GDP deflator index estimated by the World Bank, Tajikistan's GDP increased 5-fold

ha eliminato: The reported monetary and human losses were collected with the support of the local partners. Although affected by large uncertainties, these are the only datasets available for model calibration, as presented below.¶

ha eliminato: 4

ha eliminato: 3

ha formattato: Tipo di carattere: Non Corsivo

Formattato: Titolo 2

Codice campo modificato

Codice campo modificato

ha eliminato: 4

ha eliminato: 11

ha eliminato: ¶

ha eliminato: Losses in the

ha spostato (inserimento) [1]

ha eliminato: For a single flood event, occurred in Hamadoni, Tajikistan, in 2005, reported losses, flood footprints, and river flow time series were available (Saidov et al., 2006). The availability of such data allowed for the validation of some of the components of the present model, although limited to only one event. Nevertheless, and despite the caveats of carrying out a validation of a model against a single observation, showing the performances of the risk model for such event has an informative value, and is presented in the Results section.

from 2005 to 2022. However, in Tajikistan, historically high inflation has been compensated by the loss of value of the local currency (somoni) relative to the US dollar. The International Monetary Fund estimates a real GDP growth of 20% from 2005 to 2022, which, applied to the Hamadoni flood losses, would yield a range of 8.4-12 M USD, which is still well in agreement with the model results.

6 Results

6.1 Hydrological model

Table 4 shows summary performance metrics (correlation and percent bias on annual maximum streamflow) for the stations where observed streamflow was available.

Table 4. Summary performance metrics (correlation and percent bias on annual maximum streamflow).

Station	Correlation	Percent bias
KAZ_158	0.12	-16
KAZ_160	0.34	19
KAZ_161	0.62	3
KAZ_165	0.72	9
KAZ_166	0.72	2
KAZ_172	0.30	14
KAZ_232	0.85	-11
KAZ_233	0.39	-55
KAZ_234	0.56	-7
KAZ_235	0.33	-18
KAZ_238	0.72	-7
KAZ_227	0.43	8
KAZ_228	0.73	13
KAZ_245	0.62	-51
KAZ_247	0.16	-36
KAZ_46	0.68	2
KAZ_207	0.55	-47
KAZ_208	0.60	-9
KAZ_241	0.70	-156
KAZ_4	0.05	-2
UZB_41	0.71	11
UZB_10	0.75	9
KAZ_209	0.50	-3
KAZ_211	0.28	-7
KAZ_219	0.39	-30
KGZ_1	0.19	-6
KGZ_2	0.38	-1
KGZ_4	-0.38	12
UZB_6	-0.15	8
UZB_26	0.07	11

ha eliminato: ¶

ha eliminato: ¶

¶

ha eliminato: , especially as detailed flood depth maps are rare. Such maps enable the reduction of the uncertainty in the estimation the water depth estimates, so that any discrepancy between observed and modelled losses can be more clearly attributed to the vulnerability or the exposure components of the risk model. In Central Asia unfortunately only one historical flood event has these characteristics (flood depth map and post-event loss assessment), namely the 2005 Hamadoni flood in Tajikistan (Saidov et al., 2006).¶

ha eliminato: 5

ha eliminato: 5.1 Calibration and validation¶

ha eliminato: 5

ha eliminato: .1

ha eliminato: y/flood

ha eliminato: The TOPKAPI-X model was calibrated through a trial-and-error procedure adapting the initial model parameters in order to match the available observed discharge. We mainly based the model calibration on the historical daily data, but also used the annual maxima for the areas where daily data were not available. The calibration process focused mainly on robustly reproducing the flow peaks. This is because the hydrological simulations aim at estimating the extreme discharge value distributions at river sections across the region that are used to derive the flood footprint at different return periods via the hydraulic model. Since a physically based model better reproduces the flow peaks if all the other hydrological components are well represented, we made sure that the main hydrological processes were also correctly reproduced, with particular attention to the snow accumulation/melting component, which is the driver of most of the floods in this region. The calibration has been performed independently for each catchment where historical data were available. Given the distributed and physically based nature of the TOPKAPI-X hydrological model, the calibration process was not based on an automatic procedure but on the use of reasonable values of the physical parameters. This procedure allows the identification of model parameters values that provide reasonable outputs across the entire catchments, avoiding under- or over-fitting any of the available historical records. During the extreme value analysis calibration process, the main limitations of the hydrological model application were considered:¶
Absence of lake/reservoirs modeling. The influence of lakes and reservoirs was taken into account by allowing an overestimation of the flood peaks and underestimation ... [10]

ha eliminato: Table 3

ha eliminato: 3

ha formattato: Inglese (Regno Unito)

ha formattato: Inglese (Regno Unito)

ha formattato: Inglese (Regno Unito)

Tabella formattata

ha formattato: Inglese (Regno Unito)

ha formattato: Inglese (Regno Unito)

ha formattato: Inglese (Regno Unito)

6.2 Flood hazard

6.2.1 Hazard maps

The fluvial flood hazard maps for the current climate conditions have been computed over the entire Central Asia area and specifically for the five countries of Kazakhstan, Kyrgyz Republic, Uzbekistan, Tajikistan, and Turkmenistan for the selected eight return periods of 5, 10, 20, 50, 100, 200, 500, 1000 years. Two sets of fluvial flood hazard for current climate conditions were computed, namely for the undefended and defended scenarios. Figure 7 and Figure 8 show some of the resulting hazard maps for a return period of 100 years.

The comprehensive collection of the computed results of the flood hazard model can be found here: https://datacatalog.worldbank.org/search?q=SFRARR&sort=&start=0.

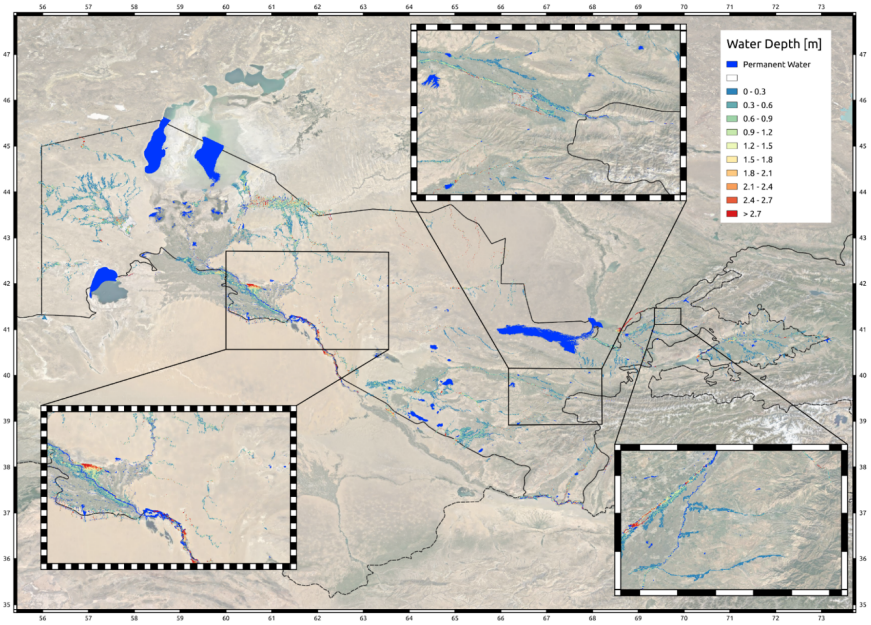

Figure 7. Fluvial flood hazard map for Uzbekistan, 100-year return period, undefended scenario. The background shades are from the MERIT DEM.

ha eliminato: Figure 7 shows observed (blue line) and TOPKAPI-X simulated (red line) discharge for a series of relevant catchments and locations, along with temperature and precipitation records. As expected, the presence of reservoirs and lakes has a clear impact on the simulation performance: the sites of Turkmenabat and Kerki (former Atamurat) on the Amu Darya River for example, are located downstream a series of reservoirs, which are not modeled in TOPKAPI-X because of lack of data. This causes the model to overestimate discharge in spring/summer when the reservoirs retain part of the snowmelt, and underestimate discharge in the rest of the year, as the reservoirs is slowly released (Figure 7). A similar behavior is observed at the Semiyarskoje and Chirchik sites on the Irtysh and the Syr Darya rivers, respectively. The two stations are located downstream of a lake (Zajsan lake's area is 1.810 km^2, Charvak lake's is 40 km^2), which explains the shift and delay in streamflow which is not equally observed in the respective catchment's upstream sites. The station at Kushum (Ural river) is located within an alluvial plain, whose lamination effect cannot be entirely reproduced by the TOPKAPI-X model and we allowed the model to overestimate the peaks and underestimate the recession curves. At stations Orenburg (Ural river) and Ulba Perevalochnaya (Amu Darya river), where these limitations do not apply, the model effectively reproduces discharge patterns throughout the entire period.¶
From an inspection of Figure 8, which shows a comparison of observed and simulated maximum flows for a series of selected sites, it is apparent that the TOPKAPI-X model exhibits a favorable correlation and minimal bias in simulating annual maximum discharge for a majority of the locations. ¶
As stated above, the acknowledged limitations of hydrological modeling across such a large area (namely effects of lakes/reservoirs and alluvial plains) were addressed during the extreme value analysis, resulting in adjustments that improved alignment with available observations. This refinement facilitated the derivation of realistic input hydrographs for the hydraulic modeling component.¶
¶ ... [11]

ha eliminato: 5.1.2 Risk¶ ... [12]

ha eliminato: 5

ha eliminato: 5

ha eliminato: Given the premises described in the previous section, it is reasonable to assert the robustness of the fluvial flood hazard maps. Naturally, future improvements in the quality and quantity of the available input datasets along with advancements in digital elevation resolution, are expected to help reducing the uncertainty further.¶

ha eliminato: Figure 5Figure 12

ha eliminato: Figure 6Figure 13

ha eliminato: 512

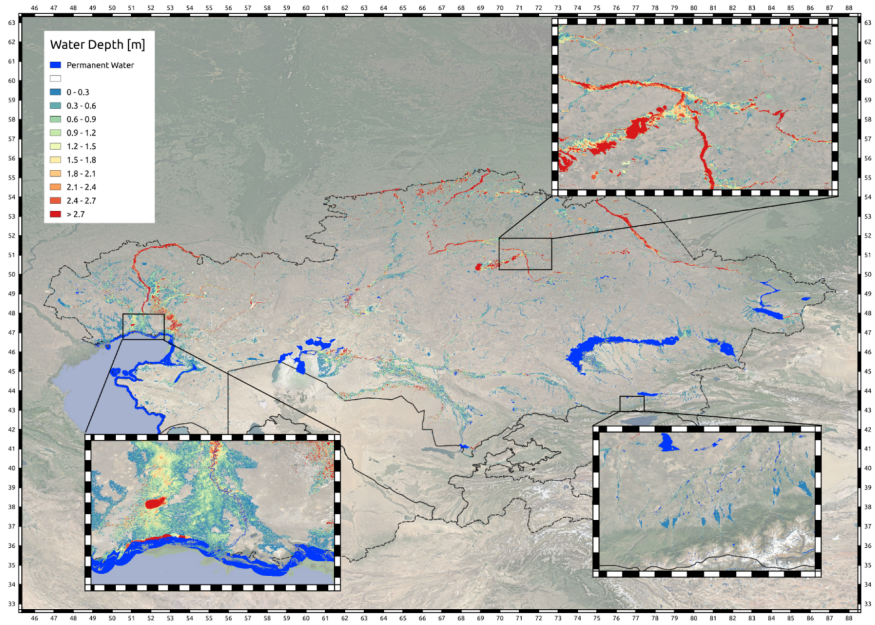

Figure 8. Fluvial flood hazard map for Kazakhstan, 100-year return period, undefended scenario. The background shades are from the MERIT DEM.

6.2.2 Hazard curves for selected target cities

Figure 9 shows the derived fluvial flood hazard curves for undefended conditions for five selected locations within the urban areas of the main flood-prone cities of the target countries: Turkmenabat, Tashkent, Dushanbe, Astana (previously Nur Sultan), Bishkek.

ha eliminato: 613

ha eliminato: 5

ha eliminato: Figure 7Figure 14

ha formattato: Inglese americano

ha eliminato: Nur Sultan

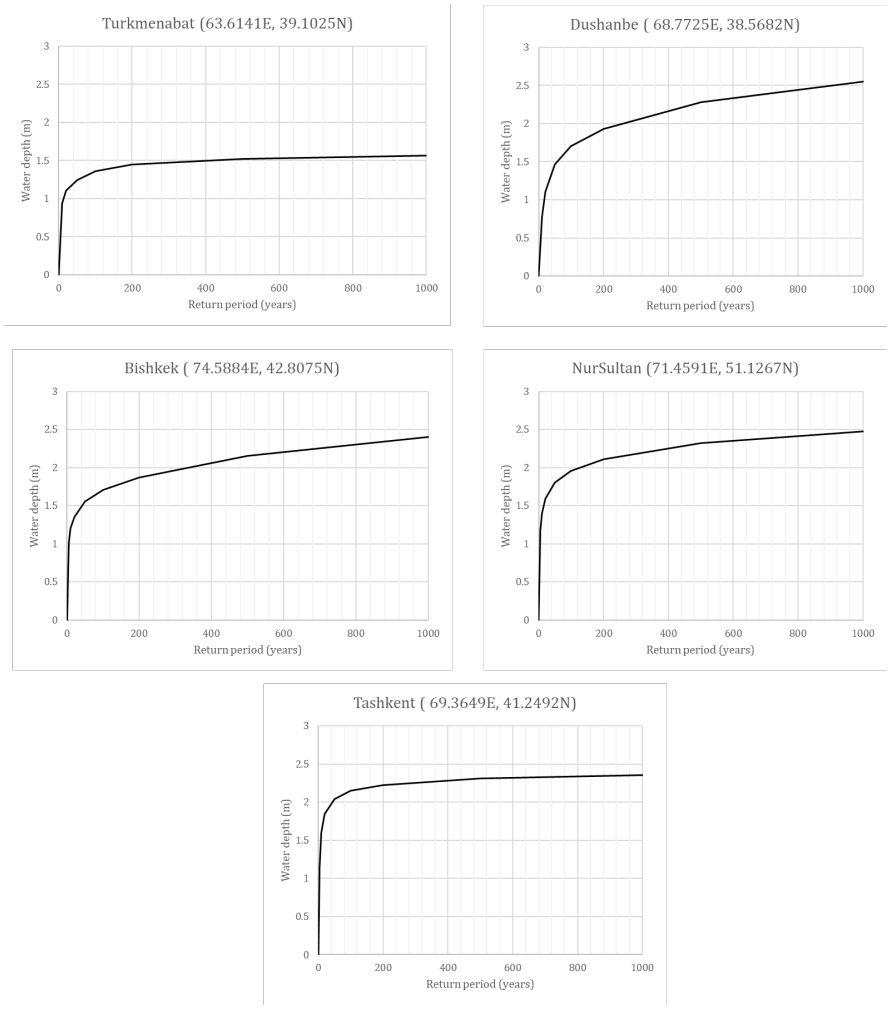

Figure 9. Undefended flood hazard curves computed at five selected target sites

6.3 Flood risk

Risk metrics

The results of the flood risk assessment are presented in terms of a loss exceedance probability curve (EP curve) and by the year loss tables (YLTs), disaggregated at administration units 1 (ADM1, which is equal to Oblast level) and administration unit 0 (ADM0, which is equal to country level). Furthermore, return period loss estimates and Average Annual Loss (AAL) at ADM1 and ADM0 levels, and for the whole region are provided in tabular format for the same eight return periods ranging from 5 to 1000 years reported earlier. In addition, for preparedness and mitigation plans it is important to estimate the possible losses (economic and human) that scenario events may cause to the current exposure. The loss results have been derived both in terms of expected values and their confidence intervals. Finally, exposure levels to various hazard intensity thresholds have been assessed for

ha eliminato: 714

ha eliminato: 5

ha spostato in alto [1]: Losses for the Hamadoni event are estimated to be in the order of 7 to 10 M USD (Saidov et al., 2006). The model presented in this paper estimated losses of 10 M USD, which shows a very good agreement between modelled and reported losses. However, the present model has been set up considering 2022 prices and exposure, while the reported losses refer to 2005 prices and exposure, and therefore this value must be corrected to account for such factors. A simple way to do this is to account for price inflation and changes in exposure using Gross Domestic Product (GDP) as a proxy. Changes in GDP in time are indeed a measure of the changes of the economy of a country. According to the GDP deflator index estimated by the World Bank, Tajikistan's GDP increased 5-fold from 2005 to 2022. However, in Tajikistan, historically high inflation has been compensated by the loss of value of the local currency (somoni) relative to the US dollar. The International Monetary Fund estimates a real GDP growth of 20% from 2005 to 2022, which, applied to the Hamadoni flood losses, would yield a range of 8.4-12 M USD, which is still well in agreement with the model results.¶

ha eliminato: 65.3.1 Calibration/validation¶

ha eliminato: *Model calibration: EP loss curves*¶
After calibration, we compared the EP loss curves for those Oblasts where partial historical loss data were available for some events (Table 3). This procedure consisted of verifying that the reported losses for the 8 historical floods were coherent with the results, by Oblast, in terms of the EP curves (i.e., reviewing that there were no systematic under- or over-estimation of losses). Figure 11 shows one of the results of these comparisons.¶
Table 3. Reported economic losses for flood events and identification of the oblast where it occurred.¶
Event ... [13]

ha eliminato: ¶

ha eliminato: ¶
65.3.2 Risk Assessment¶
¶
The flood risk results were computed following the risk assessment methodology previously described. Although this article discusses only the flood-induced losses, as alluded to before this effort was part of a multi-hazard risk assessment study that included also assessing risk for earthquakes (for the earthquake risk assessment please refer to Salgado et al. (2023). To compare the risk across different perils, it was necessary to use a peril-agnostic assessment methodology such as that adopted in CAPRA, which uses a common representation of the disaster risk assessment components, i.e., hazard, exposure, and vulnerability. Since the ... [14]

ha eliminato: *5.3.1*

ha formattato: Tipo di carattere: Corsivo, Sottolineato, Inglese americano

Formattato: Normale

ha eliminato: To be consistent with the hazard and representative of scenarios that may actually strike the five capitals of these countries, these as-if scenarios were selected based on the results of the earthquake hazard disaggregation and the flood hazard analyses.

ha formattato: Nessuna sottolineatura

population, key industrial sites, critical infrastructure, and supply infrastructure. These results are available for the current conditions (year 2020) and future (2080) scenarios considering three different projections to year 2080: the three Shared Socio-Economic Pathways SSP1, SSP4 and SSP5 considered in the exposure model development (presented in detail in Scaini et al., 2023). The future exposure only considers the residential sector. Losses have been calculated for physical risk (monetary) and human risk (fatalities).

Probabilistic flood risk results

Table 5 shows the fluvial flood risk results (undefended case) at national and regional levels in absolute and relative (to the total replacement cost of the exposure dataset) terms for the current exposure scenario. The highest absolute fluvial risk is found to be in Kazakhstan and Uzbekistan. However, when assessed in relative terms, Kazakhstan, Tajikistan and Turkmenistan have similar risk values with an AAL above 2‰. The same results for the defended case shown in highlight a large risk reduction especially for Kazakhstan, Turkmenistan and Uzbekistan. Table 7 shows the fluvial flood risk results at country and regional levels (undefended case) for one of the three different projected scenarios with consideration of the effect of climate change. The aforementioned tables use the country ISO3 codes: KGZ [Kyrgyz Republic], KAZ [Kazakhstan], TJK [Tajikistan], TKM [Turkmenistan], and UZB [Uzbekistan].

The most substantial variations among the examined scenarios stem from whether flood defenses are factored in or not, revealing more consistent disparities. In contrast, the influence of climate change, while noteworthy, exhibits greater variability depending on the specific geographical context. The exposure dataset used in the flood risk assessment for the 2080 projection only includes the residential sector, although in terms of absolute losses, the differences between the current scenario (that includes all lines of business) and the 2080 scenario (only residential assets) are not as large.

As a general comment on the estimate of flood losses, it appears that the exceedance probability curves tend to saturate relatively quickly (i.e., the slope of the curve is decreasing sharply with increasing frequency). There are three factors contributing to the quick saturation of the EP curves, one related to the hazard, another to the vulnerability, and a third one to the reproduction of flood defenses. First, flood depth hazard curves (i.e., relationships between flood depth and frequency) in this region often have a rather "flat" shape (i.e., the increase in flood depth with frequency is gradually smaller with high frequency); this phenomenon is typical of frequently inundated flat areas where floods are rather common, but the difference between water depths for small intensity and high intensity events is not that large, due to the fact that large alluvial floodplains provide plenty of space for water propagation. Second, the flood vulnerability curves developed for this project typically saturate at 30%-40%-50% of the total exposed value, mainly because they represent asset classes that bundle together buildings with different number of stories. This means that losses after a certain water depth increase very slowly, therefore causing a saturation of the loss vs frequency curve. This is typical of losses calculated for assets spread out in large-scale regions, some of which are exposed to high flood risk and others are relatively safe. Finally, another important issue is the inclusion of flood defenses in the model: a reliable representation of the flood defenses in the model would necessarily lower the high-frequency losses. However, very little data were available to precisely reproduce the flood defenses in the region, and therefore the results of the model are considered to be conservative, especially in the high-frequency part of the EP curve. Because of the characteristics of the region (many large fluvial plains with little population) and the model (large-scale aggregation and unavailability of data regarding flood defenses), we believe that the quick saturation of the flood loss curves is justified.

Table 5. Losses for different return periods (first 9 lines) and AAL (last line) for fluvial flood risk undefended scenario at Regional and Country level. The results were computed for the 2020 total exposure.

Tr (years)	Absolute values ($Million USD)						Relative values to the total replacement cost (per mille)					
	Regional	KGZ	KAZ	TJK	TKM	UZB	Regional	KGZ	KAZ	TJK	TKM	UZB
5	$2,664.3	$130.7	$1,522.0	$242.0	$203.2	$867.2	1.60	2.31	2.72	3.25	3.69	0.94
10	$2,988.6	$156.6	$1,755.9	$292.7	$262.9	$1,037.9	1.79	2.77	3.14	3.93	4.77	1.12
25	$3,360.0	$185.6	$2,021.3	$349.7	$342.5	$1,240.2	2.01	3.28	3.62	4.70	6.22	1.34
50	$3,595.7	$205.3	$2,197.2	$381.8	$393.0	$1,380.9	2.15	3.63	3.93	5.13	7.13	1.49
100	$3,797.4	$224.0	$2,361.5	$409.5	$437.0	$1,527.5	2.27	3.96	4.22	5.50	7.93	1.65

ha eliminato: ¶

ha eliminato: 5.3.2

ha formattato: Tipo di carattere: Corsivo, Sottolineato, Inglese americano

Formattato: Normale

ha eliminato: Table 4

Codice campo modificato

ha eliminato: Table 6

ha eliminato: ¶

ha eliminato: 4

ha eliminato: Grey columns show the absolute value in USD and red columns show the relative losses in per mille.

250	$4,024.7	$241.4	$2,605.0	$449.1	$502.8	$1,760.0	2.41	4.26	4.66	6.03	9.13	1.90
475	$4,178.7	$249.7	$2,830.8	$480.4	$557.3	$1,897.5	2.50	4.41	5.06	6.45	10.12	2.05
500	$4,190.7	$250.3	$2,845.7	$483.0	$561.2	$1,908.5	2.51	4.42	5.09	6.49	10.19	2.06
1000	$4,354.0	$257.6	$3,004.5	$515.6	$610.3	$2,031.3	2.61	4.55	5.37	6.93	11.08	2.20
AAL	$2,190.9	$95.1	$1,165.6	$177.0	$123.0	$630.2	1.31	1.68	2.09	2.38	2.23	0.68

Table 6. Losses for different return periods (first 9 lines) and AAL (last line) for fluvial flood risk defended scenario at Regional and Country level. The results were computed for the 2020 total exposure.

Tr (years)	Absolute values ($Million USD)						Relative values to the total replacement cost (per mille)					
	Regional	KGZ	KAZ	TJK	TKM	UZB	Regional	KGZ	KAZ	TJK	TKM	UZB
5	$1,876.9	$124.8	$976.6	$237.6	$150.5	$612.3	1.12	2.20	1.75	3.19	2.73	0.66
10	$2,170.6	$150.0	$1,200.6	$288.3	$207.2	$786.7	1.30	2.65	2.15	3.87	3.76	0.85
25	$2,481.9	$179.2	$1,474.3	$345.7	$282.7	$993.5	1.49	3.16	2.64	4.64	5.13	1.07
50	$2,677.5	$197.7	$1,655.5	$378.0	$336.2	$1,126.7	1.60	3.49	2.96	5.08	6.10	1.22
100	$2,871.1	$215.7	$1,807.9	$404.2	$380.3	$1,253.2	1.72	3.81	3.23	5.43	6.90	1.35
250	$3,145.9	$232.4	$2,030.0	$445.4	$443.7	$1,435.5	1.88	4.11	3.63	5.98	8.06	1.55
475	$3,322.4	$240.7	$2,207.4	$479.2	$483.7	$1,542.6	1.99	4.25	3.95	6.44	8.78	1.67
500	$3,335.5	$241.2	$2,222.1	$482.0	$486.3	$1,550.7	2.00	4.26	3.98	6.47	8.83	1.68
1000	$3,519.0	$248.6	$2,387.8	$513.3	$522.2	$1,657.8	2.11	4.39	4.27	6.90	9.48	1.79
AAL	$1,513.7	$91.0	$726.6	$173.7	$89.40	$432.96	0.91	1.61	1.30	2.33	1.62	0.47

Table 7. Losses for different return periods (first 9 lines) and AAL (last line) for fluvial flood risk undefended scenario at Regional and Country level. 2080 SSP1 exposure (residential only).

Tr (years)	Absolute values ($Million USD)						Relative values to the total replacement cost (per mille)					
	Regional	KGZ	KAZ	TJK	TKM	UZB	Regional	KGZ	KAZ	TJK	TKM	UZB
5	$1,800.1	$122.8	$1,168.7	$44.4	$36.4	$564.7	1.59	3.81	3.47	0.80	1.83	0.82
10	$2,028.4	$146.1	$1,354.8	$53.9	$51.9	$698.5	1.79	4.54	4.03	0.97	2.61	1.02
25	$2,315.8	$169.2	$1,573.3	$63.2	$72.3	$842.0	2.05	5.25	4.67	1.13	3.63	1.23
50	$2,512.8	$183.4	$1,730.6	$69.3	$90.5	$942.9	2.22	5.69	5.14	1.24	4.55	1.37
100	$2,705.4	$197.1	$1,884.7	$74.9	$105.5	$1,055.4	2.39	6.12	5.60	1.34	5.30	1.54
250	$2,928.1	$211.7	$2,121.0	$81.4	$123.6	$1,196.8	2.59	6.57	6.30	1.46	6.21	1.74
475	$3,054.5	$221.6	$2,267.7	$85.1	$134.9	$1,267.2	2.70	6.88	6.74	1.53	6.78	1.85
500	$3,062.7	$222.3	$2,276.5	$85.3	$135.9	$1,271.9	2.71	6.90	6.76	1.53	6.82	1.85
1000	$3,174.3	$232.2	$2,390.9	$87.7	$147.7	$1,335.3	2.81	7.21	7.10	1.57	7.42	1.94
AAL	$1,432.2	$78.2	$884.8	$29.5	$23.8	$416.2	1.27	2.43	2.63	0.53	1.20	0.61

Some of the relative losses computed for the current (2020) and future (2080) scenarios are plotted in Figure 10, Figure 11, and Figure 12. The risk reduction immediately apparent when comparing the results of Figure 10 and Figure 11 is due to the inclusion of flood defenses.

ha formattato: Nessuna sottolineatura

ha eliminato: The graphical representation of the results of Table 4 is shown in Figure 15 (return period losses: absolute values to the left, relative values to the total replacement cost in the center; AAL absolute values to the right).¶

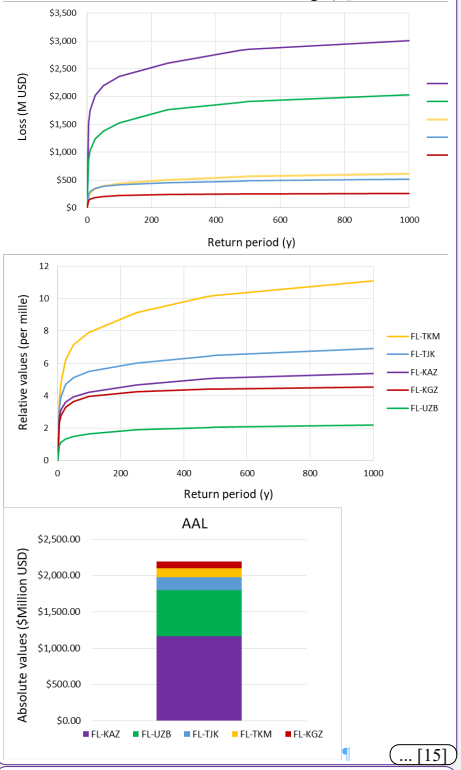

... [15]

ha eliminato: Table 4 is shown in Figure 15 (return period losses: absolute values to the left, relative values to the total replacement cost in the center; AAL absolute values to the right).¶ ... [16]

ha eliminato: Figure 15 (return period losses: absolute values to the left, relative values to the total replacement cost in the center; AAL absolute values to the right).¶ ... [17]

ha eliminato: The graphical representation of the results of Table 5 is shown in Figure 16 (return period losses: absolute values to the left, relative values to the total replacement cost in the center; AAL absolute values to the right).¶ ... [18]

ha eliminato: 6

ha eliminato: Grey columns show the absolute value in USD and red columns show the relative losses in per mille.

ha eliminato: Figure 10Figure 17

ha eliminato: Figure 11Figure 18

ha eliminato: Figure 12Figure 19

ha eliminato: Figure 10Figure 17

ha eliminato: Figure 11Figure 18

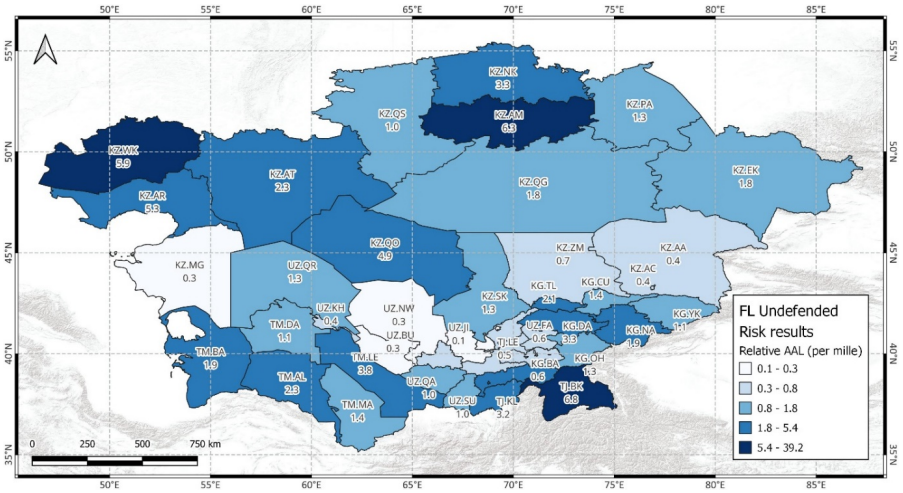

Figure 10. Current (2020) exposure and undefended scenario: relative losses. Background grey shades from the MERIT DEM.

ha eliminato: 1017

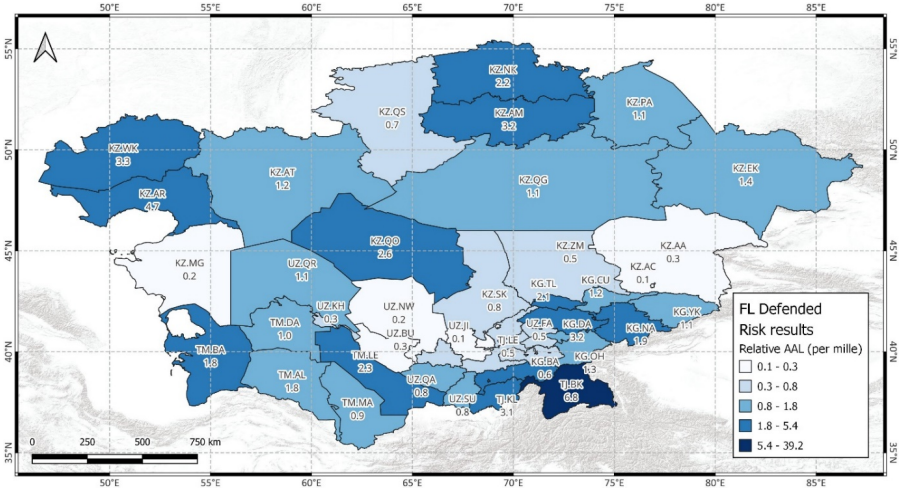

Figure 11. Current (2020) exposure and defended scenario: relative losses. Background grey shades from the MERIT DEM.

ha eliminato: 1118

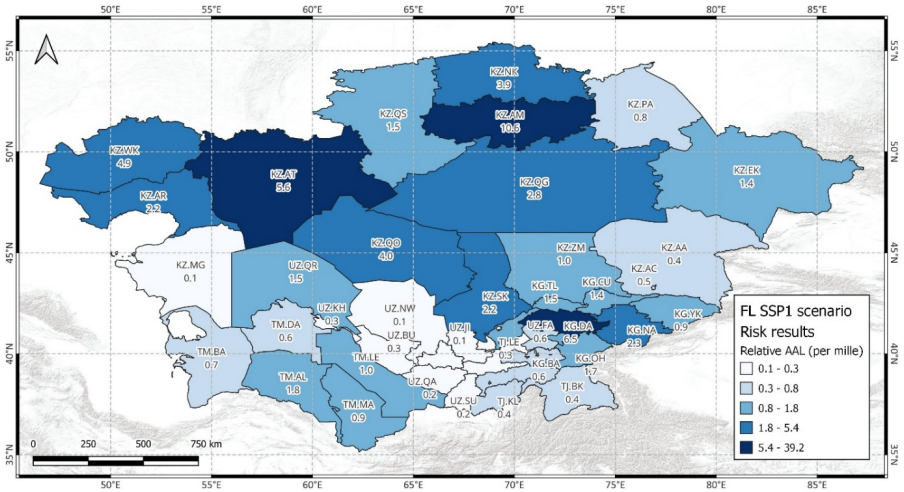

Figure 12. Future (2080) exposure and Climate Change – SSP1 scenario: relative losses

For the undefended scenario, the largest relative AALs are found in Kazakhstan and Tajikistan, with values above 6‰. In the five considered countries, the largest relative AALs by sector are found for the transport and agricultural sector (the two types of crops included in this assessment: cotton and wheat). For the case of cotton crops, the largest relative AALs are found in Kazakhstan, Turkmenistan, and Tajikistan with values above 6‰. Regarding flood risk fatalities, the highest risk is found, as expected, for the undefended case. The largest values are found for the Akmolinskaya Oblast in Kazakhstan and Khatlon Province in Tajikistan. On average, at Oblast level, there is a decrease of 20% of flood fatalities' risk in the defended case. Regarding future scenarios, and considering climate change, there is a variable trend at Oblast level for the flood fatality risk, although consistent among the considered SSPs. In general, risk values in future scenarios are increased by a factor between 1.5 and 2.0, such as in the following Oblasts: Sirdarya (Uzbekistan), Ysyk-Kol, and Jalal-Abad in the Kyrgyz Republic and Turkistan and Karagandiskaya in Kazakhstan. However, there are extreme cases, such as the Mangistauskaya Oblast in Kazakhstan, where the risk increases by seven times. Conversely, there are Oblasts, such as Lebap (Turkmenistan), Khatlon Province (Tajikistan), Samarkand (Uzbekistan) and Batken (Kyrgyz Republic), for which decreases between 80 and 90% are observed for all SSPs.

As expected, flood risk is lower for the defended case although caution should be used when interpreting these results due to the assumptions about flood defenses' location and height discussed earlier. That being said, a comparison between the two cases at Oblast level can be made and some discussion is provided next. Overall, the Oblast with the largest flood AAL is the Badakhshan Autonomous Mountainous Region in Tajikistan. The largest relative difference caused by modelling or not the flood defenses is found in Batken Oblast (Kyrgyz Republic), although for the undefended case the flood risk AAL was relatively low (0.4‰). A major flood risk reduction due to the inclusion of the defenses is observed in Ysyk-Kol Oblast, with a decrease of around 40%, which is a significant decrease considering the large flood risk AAL for the undefended case.

7 Discussion

This study presents the first high-resolution, regional-scale, transboundary fully probabilistic risk assessment for the area, providing decision-making aids and disaster risk management resources. Notably, the involvement of local stakeholders and unprecedented access to local data enhance its significance.

Within the SFRARR project, multiple workshops and meetings with local stakeholders and experts were held. In particular, eight capacity building workshops devoted to the different risk assessment components, namely five country-based workshops on exposure assessment and three regional thematic workshops on hazard, vulnerability and risk modelling. This activity was carried out in close collaboration with local experts and representatives from

ha eliminato: 1219

ha eliminato: ,

ha eliminato: As previously stated, these results are part of a multi-hazard risk assessment study including both earthquake and flood risk. Combined results (earthquake and undefended flood), show that there are Oblasts such as JalalAbad (in the Kyrgyz Republic), and Khatlon Province and the Cities and Districts of the Republican Subordination (in Tajikistan) where the risk caused by these two hazards is high. On the other hand, there are Oblasts where only the risk caused by one of these hazards is relevant whereas the other is very low, as in the case of Zapadno-kazachstanskaya (in Kazakhstan) where the undefended flood relative AAL is almost 6‰ and earthquake relative AAL is approximately 0.1‰, or the case of Almatinskaya Oblast (in Kazakhstan) where earthquake relative AAL is above 2‰ but undefended flood relative AAL is lower than 0.5‰. Similar results can be observed for the Sughd Province (Takikistan) and Namangan (Uzbekistan) with large and low relative AALs for earthquakes and floods, respectively, or for Karakalpakstan (Uzbekistan), Lebap (Turkmenistan) and Akmolinskaya (Kazakhstan), with large and low relative AALs for floods and earthquakes, respectively (for further details on the earthquake risk assessment please refer to Salgado et al. (2023).¶

ha eliminato: 6

all five countries. The workshops provided participants an opportunity to learn about international best practice and latest methodologies related to natural risks assessment. These workshops allowed sharing knowledge with local experts and provided an opportunity for emergence and inclusion of a greater amount of locally collected information into the analysis. Obtaining daily discharge and hydraulic protection data from local sources proved complex due to variability in data quality and form. Compiling comprehensive hydraulic protection data at the country level was hindered by its highly classified and confidential nature, posing challenges for acquisition.

In terms of model performance, when comparing the reported losses with the EP curves (in terms of return periods), we observe that for the case of the Khatlon Oblast in Tajikistan the April 2006 flood is associated with a return period of approximately 650 years, the July 2005 flood is associated with a return period of approximately 20 years., whereas floods with lower reported losses, such as the April 2014, and May 2021 have a return period of approximately two years. The May 2010 flood corresponds to the event with the largest reported losses, and as per the EP curve calculated for this Oblast, has a return period longer than 1000 years. Since the Khatlon Oblast has experienced an exceptional number of reported events in the past 20 years, which is uncommon in the rest of the regions, it is reasonable to assume some of the reported events are associated to such short return periods. Furthermore, note that, strictly speaking the comparison between Oblast-wide losses and event-specific losses for the purpose of assessing the reasonability of the associated return periods is not correct. Small events only affect a portion of the Oblast and other events might have happened during the same year. Therefore, the yearly Oblast losses are, intuitively, larger than event-specific losses that may have occurred in that year. Hence, we expect that small, localized events are associated to short Oblast-scale loss return periods. On the other side of the spectrum, the large May 2010 event in the Khatlon province appears to be out of the limits of the exceedance probability curve. However, it must be noted that there is a large discrepancy among the different data sources in the reported losses for this event: SwissRe reported a loss of around 200 M USD, whereas AON around 5 M USD. The overestimation of observed losses by one of the sources (or perhaps the inclusion of losses by landslides and mudslides, which are not included in this model) might be the cause of the very long estimated return period. In any case, referring to the event above, the chance that a 10,000yr loss or larger has been observed in 20 years is very small. This rare event can be explained by the discrepancy in the reported losses but, in general, such extremely large losses associated with very long return periods are not tenable. This is the reason why we calibrated the model to eliminate such cases After calibration, the reported event loss values have plausible return periods when compared to the modeled losses from the subnational EP curves.

ha eliminato: ¶

ha eliminato: ¶

ha formattato: Inglese americano

Hereafter, we delineate a series of strengths and limitations inherent to this risk assessment.

7.1 Strengths

ha eliminato: 6

- A main strength of this risk assessment is that a peril-agnostic methodology was used, facilitating the comparison of results across country, sector, and hazards (earthquake and flood). This was achieved by using the same representation for all the key risk components and by computing the same risk metrics using the same probabilistic approach.
- This is the first study in the region that disaggregates flood risk results into subnational level (Oblast), national level (country), and regional level (five countries), providing a complete disaster risk estimation and results compatible with the overall objectives of the project.
- The regional approach adopted for carrying out this risk assessment used consistent assumptions, modelling approaches and treatment of uncertainties. This is key considering that the final objective of this study is the regional calculation of losses caused by floods of different types (pluvial, flood not shown here) and different kind of events (earthquakes).
- This is the first project in the region that considers a complete exposure dataset for the estimation of flood risk. Besides buildings (considered in previous studies), other relevant types of assets, such as the transportation infrastructure (roads and bridges) and key crops (cotton and wheat) have been included too.
- Given that the software utilized to estimate the physical and human losses has a friendly graphic user interface and some GIS capabilities, the obtained flood risk results are expected to facilitate the capacity building process in disaster risk assessment in Central Asia.

ha eliminato: The earthquake losses are discussed in detail in Salgado et al. (2023).

ha eliminato:

- The risk results obtained in this study provide losses for floods at subnational level with a reasonable level of accuracy. This has been achieved using a good amount of local data for hazard modeling and risk validation and adopting a high-resolution approach to the modeling of the hazard and exposure components.
- By having developed an exposure dataset with different lines of business, all the loss results can be disaggregated by categories. This information is valuable to different stakeholders at subnational to regional levels.
- The level of detail paid to most components of the flood risk model is higher than that adopted in previous studies carried out in the region. The refined approach has been complemented by the inclusion of additional lines of business in the exposure datasets, an addition that enabled the derivation of a more comprehensive picture of the flood risk in the region.

7.2 Limitations

ha eliminato: 6

- Hydrological model calibration: absence of lake/reservoirs in the model. The influence of lakes and reservoirs was taken into account by allowing an overestimation of the flood peaks and underestimation of the low flows for downstream stations of primary reservoirs. These reservoirs effectively attenuate flood waves by storing water during peak events and releasing it during drier periods. This behavior was not explicitly modeled due to lack of information on the reservoir management strategies. Hence, it was anticipated that the model would not precisely replicate observed hydrographs for stations located downstream of reservoirs (e.g., the Turkmenabat, Kerki (former Atamurat), Semiyarskoje and Chirchik stations in). This issue was dealt with by correcting the extreme value flow distributions downstream reservoirs based on the available observations.

Codice campo modificato

- Inability to reproduce the effect of alluvial plains, which similarly to reservoirs alter flood waves by flattening peak flows. To address this, the same approach was adopted as with reservoirs, namely we allowed the overestimation of the peaks and the underestimation of recession curves (e.g, evident at stations like the Kushum and Gram in) for stations located within alluvial plains. This issue was dealt with by correcting the extreme value flow distributions in alluvial plains based on the available observations.

Formattato: Paragrafo elenco;References;Main numbered paragraph;List Paragraph (numbered (a));Normal 2;List_Paragraph;Multilevel para_II;List Paragraph1;Numbered List Paragraph;Bullets;Colorful List - Accent 11;123 List Paragraph;Body;Bullet;Normal 2 DC;Liste 1, SpazioDopo: 6 pt, Interlinea: multipla 1.1 ri, Puntato + Livello:1 + Allinea a: 0.63 cm + Imposta un rientro di: 1.27 cm

Codice campo modificato

- The hazard model is not supported by the level of detail and accurate data that are often available when developing national and sub-national scale models in other regions. However, until those more detailed analyses are performed and made available to the public (https://datacatalog.worldbank.org/search?q=SFRARR&sort=&start=0), these risk estimates can certainly be used as first-order quantification of risks. These risk estimates are certainly suitable both to support raising awareness on this topic, and to guide the development of more refined analyses with the same probabilistic framework adopted here.
- Catastrophe risk models always have an associated level of uncertainty even when developed for the current hazard and exposure characteristics. In this project, a projection of exposure was performed to year 2080 (for the residential sector only) for different Shared Socio-Economic Pathways (SSPs) for one climate change scenario. These results are intended to be indicative and useful for comparison purposes only. The relative results should be preferred over the absolute losses.
- The risk estimates should not be used as the only support for planning and designing specific risk management infrastructure. These applications should be informed by flood risk studies for specific areas that utilize a more comprehensive set of input data such as those confidential and highly classified datasets available to the central governments.

8 Conclusions

ha eliminato: 7

This article presented the methodological framework utilized for developing a fully probabilistic flood risk assessment for Kazakhstan, Kyrgyz Republic, Tajikistan, Turkmenistan and Uzbekistan in Central Asia and the obtained risk estimates. The results are expressed in terms of EP curves, AAL and specific return period losses, which are the metrics commonly used to shape different disaster risk management strategies. The risk assessment study includes several variants of the hazard (current and future including climate change conditions) and exposure components (current all lines of business and future, residential line only, for different Shared Socio-Economic

Pathways). The results of the risk assessment are of general use but were intended primarily to inform World Bank's engagement in supporting regional and national disaster risk financing and insurance applications, including traditional and parametric solutions for the structuring of a regional risk mitigation program. These risk estimates can be used by the World Bank to initiate a policy dialogue with the governments of Kazakhstan, Kyrgyz Republic, Tajikistan, Turkmenistan and Uzbekistan.

Acknowledgements

This study has been carried out within the framework of the World Bank-funded project "Strengthening Financial Resilience and Accelerating Risk Reduction in Central Asia" (SFRARR). The authors would like to thank all the local experts involved in the project tasks and the participants to the workshops organised within the SFRARR project for their contribution to the implementation of the flood risk model presented in this paper. The constant support of Dr. Sergey Tyagunov in all project tasks was greatly appreciated.

Competing interests

The contact author has declared that none of the authors has any competing interests.

Data availability

The technical reports produced during the SFRARR project, containing detailed explanations of the work carried out during the fully probabilistic flood risk assessment, are available upon request to the corresponding author.

Author Contributions

GC, GB, SD: conceptualization, validation, risk assessment methodology, formal analysis, writing review and editing. PC: conceptualization, data collection, validation, writing and editing. PB: risk assessment methodology, validation, calibration, writing review and editing; MM, EF, MO: conceptualization, risk assessment methodology. CA, BH, OG: software, risk assessment. ZR, KA, SM, VI: data collection, calibration, validation. VB: data collection, calibration, validation, writing review.

References

Alfieri, L., Salamon, P., Bianchi, A., Neal, J., Bates, P., and Feyen, L.: Advances in pan-European flood hazard mapping, Hydrol. Process., 28, 4067–4077, https://doi.org/10.1002/hyp.9947, 2014.

Arcement, G.J., and Schneider, V.R.: Guide for selecting Manning's roughness coefficients for natural channels and flood plains. Vol. 2339. Washington, DC: US Government Printing Office, 1989.

Asian Development Bank: Tajikistan: Khatlon Province Flood Risk Management Project, 2015.

Baky, M. A. Al, Islam, M., and Paul, S.: Flood Hazard, Vulnerability and Risk Assessment for Different Land Use Classes Using a Flow Model, Earth Syst. Environ., 4, 225–244, https://doi.org/10.1007/s41748-019-00141-w, 2020.

Bates, P. D.: Flood Inundation Prediction, Annu. Rev. Fluid Mech., 54, 287–315, https://doi.org/10.1146/annurev-fluid-030121-113138, 2022.

Bates, P. D., Horritt, M. S., and Fewtrell, T. J.: A simple inertial formulation of the shallow water equations for efficient two-dimensional flood inundation modelling, J. Hydrol., https://doi.org/10.1016/j.jhydrol.2010.03.027, 2010.

Bloemendaal, N., Haigh, I. D., de Moel, H., Muis, S., Haarsma, R. J., and Aerts, J. C. J. H.: Generation of a global synthetic tropical cyclone hazard dataset using STORM, Sci. Data, 7, 40, https://doi.org/10.1038/s41597-020-0381-2, 2020.

Bubeck, P., de Moel, H., Bouwer, L. M., and Aerts, J. C. J. H.: How reliable are projections of future flood damage?, Nat. Hazards Earth Syst. Sci., 11, 3293–3306, https://doi.org/10.5194/nhess-11-3293-2011, 2011.

CAC DRMI: Risk assessment for Central Asia and Caucasus: desk study review, 2009.

ha formattato

Ciarapica, L. and Todini, E.: TOPKAPI: a model for the representation of the rainfall-runoff process at different scales, Hydrol. Process., 16, 207–229, https://doi.org/10.1002/hyp.342, 2002.
Courant, R., Friedrichs, K., and Lewy, H.: Über die partiellen Differenzengleichungen der mathematischen Physik, Math. Ann., 100, 32–74, https://doi.org/10.1007/BF01448839/METRICS, 1928.
Dottori, F. and Todini, E.: Developments of a flood inundation model based on the cellular automata approach: Testing different methods to improve model performance, Phys. Chem. Earth, Parts A/B/C, 36, 266–280, https://doi.org/10.1016/j.pce.2011.02.004, 2011.
Dottori, F., Figueiredo, R., Martina, M. L. V., Molinari, D., and Scorzini, A. R.: INSYDE: a synthetic, probabilistic flood damage model based on explicit cost analysis, Nat. Hazards Earth Syst. Sci., 16, 2577–2591, https://doi.org/10.5194/nhess-16-2577-2016, 2016.
Dottori, F., Martina, M. L. V., and Figueiredo, R.: A methodology for flood susceptibility and vulnerability analysis in complex flood scenarios, J. Flood Risk Manag., 11, S632–S645, https://doi.org/10.1111/jfr3.12234, 2018.
EM-DAT CRED: 2010. The OFDA/CRED international disaster database. Université catholique., 2010.
Fang, G. H., Yang, J., Chen, Y. N., and Zammit, C.: Comparing bias correction methods in downscaling meteorological variables for a hydrologic impact study in an arid area in China, Hydrol. Earth Syst. Sci., 19, 2547–2559, https://doi.org/10.5194/hess-19-2547-2015, 2015.
FEMA: Hazus Flood Model User Guidance., 261 pp., 2018.
Figueiredo, R., Schröter, K., Weiss-Motz, A., Martina, M. L. V., and Kreibich, H.: Multi-model ensembles for assessment of flood losses and associated uncertainty, Nat. Hazards Earth Syst. Sci., 18, 1297–1314, https://doi.org/10.5194/nhess-18-1297-2018, 2018.
Francés, F., García-Bartual, R., and Bussi, G.: High return period annual maximum reservoir water level quantiles estimation using synthetic generated flood events, in: Risk Analysis, Dam Safety, Dam Security and Critical Infrastructure Management. Proceedings of the 3rd international forum on risk analysis, dam safety , dam security and critical management (3IWRDD-FORUM), Valencia, Spain, 17-18 October 2011, edited by: Escuder-Bueno, I., Matheu, E., Altarejos-García, L., and Castillo-Rodríguez, J., CRC Press, London, 185–190, 2011.
GFDRR: Europe and Central Asia Country Risk Profiles for Floods and Earthquakes, 2016.
Giandotti, M.: Previsione delle piene e delle magre dei corsi d'acqua, Ist. Poligr. dello Stato, 1934.
Giorgi, F., Jones, C., and Asrar, G.: Addressing climate information needs at the regional level: the CORDEX framework, World Meteorological Organization (WMO) Bulletin, 58(3), p.175, 2009.
Guillod, B. P. B. P., Jones, R. G. R. G., Dadson, S. J. S. J., Coxon, G., Bussi, G., Freer, J., Kay, A. L. A. L., Massey, N. R. N. R., Sparrow, S. N. S. N., Wallom, D. C. H. D. C. H., Allen, M. R. M. R., and Hall, J. W. J. W.: A large set of potential past, present and future hydro-meteorological time series for the UK, Hydrol. Earth Syst. Sci., 22, 611–634, https://doi.org/10.5194/hess-22-611-2018, 2018.
Hendrawan, V. S. A. and Komori, D.: Developing flood vulnerability curve for rice crop using remote sensing and hydrodynamic modeling, Int. J. Disaster Risk Reduct., 54, 102058, https://doi.org/10.1016/j.ijdrr.2021.102058, 2021.
Hersbach, H., Bell, B., Berrisford, P., Horányi, A., Sabater, J. M., Nicolas, J., Radu, R., Schepers, D., Simmons, A., Soci, C., and Dee, D.: Global reanalysis: goodbye ERA-Interim, hello ERA5. ECMWF newsletter 159, 17–24 pp., 2019.
Huizinga, J., de Moel, H., and Szewczyk, W.: Global flood depth-damage functions, 1–108 pp., https://doi.org/10.2760/16510, 2017.
JICA, Study on Natural Disaster Prevention in Pyanj River, https://openjicareport.jica.go.jp/pdf/11870748_01.pdf, 2007.
Kwak, Y., Shrestha, B. B., Yorozuya, A., and Sawano, H.: Rapid Damage Assessment of Rice Crop After Large-Scale Flood in the Cambodian Floodplain Using Temporal Spatial Data, IEEE J. Sel. Top. Appl. Earth Obs. Remote Sens., 8, 3700–3709, https://doi.org/10.1109/JSTARS.2015.2440439, 2015.
Lafon, T., Dadson, S. J., Buys, G., and Prudhomme, C.: Bias correction of daily precipitation simulated by a regional climate model: a comparison of methods, Int. J. Climatol., 33, 1367–1381, https://doi.org/10.1002/joc.3518, 2013.
Libert, B.: Water management in Central Asia and the activities of UNECE, Cent. Asian Waters, 35, 2008.
M.S. Saidov: ИНЖЕНЕРНО-ГЕОЛОГИЧЕСКАЯ ОЦЕНКА И ПРОГНОЗ ОПАСНЫХ ГЕОЛОГИЧЕСКИХ ПРОЦЕССОВ ТРАНСГРАНИЧНОЙ ТЕРРИТОРИИ РЕСПУБЛИКИ ТАДЖИКИСТАН И РЕСПУБЛИКИ АФГАНИСТАН (НИЖНИЙ ПЯНДЖ), 2020.
Merz, B., Aerts, J., Arnbjerg-Nielsen, K., Baldi, M., Becker, A., Bichet, A., Blöschl, G., Bouwer, L. M., Brauer, A., Cioffi, F., Delgado, J. M., Gocht, M., Guzzetti, F., Harrigan, S., Hirschboeck, K., Kilsby, C., Kron, W., Kwon, H.-H., Lall, U., Merz, R., Nissen, K., Salvatti, P., Swierczynski, T., Ulbrich, U., Viglione, A., Ward, P. J., Weiler, M., Wilhelm, B., and Nied, M.: Floods and climate: emerging perspectives for flood risk assessment and management, Nat. Hazards Earth Syst. Sci., 14, 1921–1942, https://doi.org/10.5194/nhess-14-1921-2014, 2014.
Mitchell-Wallace, K., Jones, M., Hillier, J., and Foote, M.: Natural catastrophe risk management and modelling:

ha formattato: Italiano

ha eliminato: ,…World Meteorological Organization (WMO) Bulletin, 58(3), p.175, 2009. … Organ. Bull., ... [19]

ha formattato

ha formattato ... [20]

ha formattato ... [21]

ha formattato ... [22]

A practitioner's guide, John Wiley & Sons, 2017.
Molinari, D., Scorzini, A. R., Gallazzi, A., and Ballio, F.: AGRIDE-c, a conceptual model for the estimation of flood damage to crops: development and implementation, Nat. Hazards Earth Syst. Sci., 19, 2565–2582, https://doi.org/10.5194/nhess-19-2565-2019, 2019.
Morrison, J. E. and Smith, J. A.: Stochastic modeling of flood peaks using the generalized extreme value distribution, Water Resour. Res., https://doi.org/10.1029/2001wr000502, 2002.
Mudbhatkal, A. and Mahesha, A.: Bias Correction Methods for Hydrologic Impact Studies over India's Western Ghat Basins, J. Hydrol. Eng., 23, https://doi.org/10.1061/(ASCE)HE.1943-5584.0001598, 2018.
Muñoz-Sabater, J., Dutra, E., Agustí-Panareda, A., Albergel, C., Arduini, G., Balsamo, G., Boussetta, S., Choulga, M., Harrigan, S., Hersbach, H., Martens, B., Miralles, D., Piles, M., Rodríguez-Fernández, N., Zsoter, E., Buontempo, C., and Thépaut, J.-N.: ERA5-Land: A state-of-the-art global reanalysis dataset for land applications, Earth Syst. Sci. Data Discuss., https://doi.org/10.5194/essd-2021-82, 2021.
Nachtergaele, F., Velthuizen, H. van, Verelst, L., Batjes, N., Dijkshoorn, K., Engelen, V. van, Fischer, G., Jones, A., Montanarella, L., Petri, M., Prieler, S., Shi, X., Teixeira, E., and Wiberg, D.: Harmonized World Soil Database Version 1.2. Food and Agriculture Organization of the United Nations (FAO)., 19th World Congr. Soil Sci. Soil Solut. a Chang. World, 2012.
Ozturk, T., Turp, M. T., Türkeş, M., and Kurnaz, M. L.: Projected changes in temperature and precipitation climatology of Central Asia CORDEX Region 8 by using RegCM4.3.5, Atmos. Res., https://doi.org/10.1016/j.atmosres.2016.09.008, 2017.
Pappenberger, F., Dutra, E., Wetterhall, F., and Cloke, H. L.: Deriving global flood hazard maps of fluvial floods through a physical model cascade, Hydrol. Earth Syst. Sci., 16, 4143–4156, https://doi.org/10.5194/hess-16-4143-2012, 2012.
Pielke, R.: Economic 'normalisation' of disaster losses 1998–2020: a literature review and assessment, Environmental Hazards,20:2,93-111,DOI: 10.1080/17477891.2020.1800440, 2021.
Pielke, R. Jr, Burgess, M.G., Ritchie, J.: Plausible 2005–2050 emissions scenarios project between 2 °C and 3 °C of warming by 2100, Environmental Research Letters, Volume 17, Number 2 https://doi.org/10.1088/1748-9326/ac4ebf, 2022.
Pittore, M., Bindi, D., Tyagunov, S., Wieland, M., Picozzi, M., Pilz, M., Ullah, S., Fleming, K., Parolai, S., Zschau, J., Moldobekov, B., Abdrakhmatov, K., Begaliev, U., Yasunov, P., Ishuk, A., and Mikhailova, N.: Seismic hazard and risk in Central Asia. Scientific Technical Report STR11/14. GFZ Helmholtz-Zentrum Potsdam, 17 pp., https://doi.org/https://doi.org/10.2312/GFZ.b103-11149, 2011.
Pittore, M., Haas, M., and Silva, V.: Variable resolution probabilistic modeling of residential exposure and vulnerability for risk applications, Earthq. Spectra, 36, 321–344, https://doi.org/10.1177/8755293020951582, 2020.
Pollner, J., Kryspin-Watson, J., and Nieuwejaar, S.: Disaster Risk Management and Climate Change Adaptation in Europe and Central Asia, World Bank, 1–53, 2010.
Qian, L., Chen, X., Wang, X., Huang, S., and Luo, Y.: The Effects of Flood, Drought, and Flood Followed by Drought on Yield in Cotton, Agronomy, 10, 555, https://doi.org/10.3390/agronomy10040555, 2020.
Räty, O., Räisänen, J., and Ylhäisi, J. S.: Evaluation of delta change and bias correction methods for future daily precipitation: intermodel cross-validation using ENSEMBLES simulations, Clim. Dyn., 42, 2287–2303, https://doi.org/10.1007/s00382-014-2130-8, 2014.
Räty, O., Räisänen, J., Bosshard, T., and Donnelly, C.: Intercomparison of Univariate and Joint Bias Correction Methods in Changing Climate From a Hydrological Perspective, Climate, 6, 33, https://doi.org/10.3390/cli6020033, 2018.
Reinoso, E., Ordaz, M., Cardona, O.-D., Bernal, G. A., and Contreras, M.: After 10 years of CAPRA, in: Proceedings of the 16th European Conference on Earthquake Engineering, 2018.
Reyer, C. P. ., Otto, I. M., Adams, S., Albrecht, T., Baarsch, F., Cartsburg, M., Coumou, D., Eden, A., Ludi, E., Marcus, R., Mengel, M., Mosello, B., Robinson, A., Schleussner, C.-F., Serdeczny, O., and Stagl, J.: Climate change impacts in Central Asia and their implications for development, Reg. Environ. Chang., 17, 1639–1650, https://doi.org/10.1007/s10113-015-0893-z, 2017.
Rosbjerg, D. and Madsen, H.: Uncertainty measures of regional flood frequency estimators, J. Hydrol., https://doi.org/10.1016/0022-1694(94)02624-K, 1995.
Rosi, A., Frodella, W., Nocentini, N., Caleca, F., Havenith, H. B., Strom, A., Saidov, M., Bimurzaev, G. A., and Tofani, V.: Comprehensive landslide susceptibility map of Central Asia, Nat. Hazards Earth Syst. Sci., 23, 2229–2250, https://doi.org/10.5194/nhess-23-2229-2023, 2023.
Saidov, M. S., Pilguy, Y. N., Komilov, O. K., Davlyatshoeva, L. V., and Shakirzhanova, G. N.: Flooding in Hamadoni: Causes, Consequences and Forecast, Dushanbe, 2006.
Salazar, S., Francés, F., García-Bartual, R., Ortíz, E., Múnera, J. C., and Vélez, J. J.: Flood risk assessment in a Spanish Mediterranean catchment, in: EGU General Assembly, 2009.
Scaini, C., Tamaro, A., Adilkhan, B., Sarzhanov, S., Ismailov, V., Umaraliev, R., Safarov, M., Belikov, V.,

Karayev, J., and Faga, E.: A new regionally consistent exposure database for Central Asia: population and residential buildings, Nat. Hazards Earth Syst. Sci., 24, 929–945, https://doi.org/10.5194/nhess-24-929-2024, 2024a.
Scaini, C., Tamaro, A., Adilkhan, B., Sarzhanov, S., Ergashev, Z., Umaraliev, R., Safarov, M., Belikov, V., Karayev, J., and Fagà, E.: A regional-scale approach to assessing non-residential building, transportation and cropland exposure in Central Asia, Nat. Hazards Earth Syst. Sci., 24, 355–373, https://doi.org/10.5194/nhess-24-355-2024, 2024b.
Schumann, G. J. -P., Stampoulis, D., Smith, A. M., Sampson, C. C., Andreadis, K. M., Neal, J. C., and Bates, P. D.: Rethinking flood hazard at the global scale, Geophys. Res. Lett., 43, https://doi.org/10.1002/2016GL070260, 2016.
Scussolini, P., Aerts, J. C. J. H., Jongman, B., Bouwer, L. M., Winsemius, H. C., De Moel, H., and Ward, P. J.: FLOPROS: an evolving global database of flood protection standards, Nat. Hazards Earth Syst. Sci., https://doi.org/10.5194/nhess-16-1049-2016, 2016.
Shrestha, M., Acharya, S. C., and Shrestha, P. K.: Bias correction of climate models for hydrological modelling – are simple methods still useful?, Meteorol. Appl., 24, 531–539, https://doi.org/10.1002/met.1655, 2017.
Steinschneider, S., Wi, S., and Brown, C.: The integrated effects of climate and hydrologic uncertainty on future flood risk assessments, Hydrol. Process., n/a-n/a, https://doi.org/10.1002/hyp.10409, 2014.
Tatem, A. J.: WorldPop, open data for spatial demography, https://doi.org/10.1038/sdata.2017.4, 2017.
Teutschbein, C. and Seibert, J.: Bias correction of regional climate model simulations for hydrological climate-change impact studies: Review and evaluation of different methods, J. Hydrol., 456–457, 12–29, https://doi.org/10.1016/j.jhydrol.2012.05.052, 2012.
The Global Water System Project: Global Reservoir and Dam (GRanD) Database, 2011.
The World Bank: Measuring seismic risk in Kyrgyz Republic : seismic risk reduction strategy: Working Paper123049, 244 pp., 2017.
Tsakiris, G.: Flood risk assessment: concepts, modelling, applications, Nat. Hazards Earth Syst. Sci., 14, 1361–1369, https://doi.org/10.5194/nhess-14-1361-2014, 2014.
Umaraliev, R., Moura, R., Havenith, H.-B., Almeida, F., and Nizamiev, A. G.: Disaster Risk in Central Asia: Socio-Economic Vulnerability Context and Pilot-Study of Multi-Risk Assessment in a Remote Mountain Area of Kyrgyz Republic, Eur. J. Eng. Res. Sci., 5, 234–244, https://doi.org/10.24018/ejers.2020.5.3.1772, 2020.
UNDP: Situation analysis of disaster risk assessment in Kyrgyzstan, 2014.
UNISDR: In-depth Review of Disaster Risk Reduction in the Kyrgyz Republic, 2010.
Wang, P., Huang, C., Colstoun, E. C. B. de, Tilton, J. C., and Tan, B.: Documentation for the Global Human Built-up And Settlement Extent (HBASE) Dataset From Landsat, NASA Socioecon. Data Appl. Cent., 2017a.
Wang, P., Huang, C., Brown de Colstoun, E. C., Tilton, J. C., and Tan, B.: Global Human Built-up And Settlement Extent (HBASE) Dataset From Landsat. Palisades, NY: NASA Socioeconomic Data and Applications Center (SEDAC)., https://doi.org/10.7927/H4DN434S, 2017b.
Ward, P. J., Jongman, B., Weiland, F. S., Bouwman, A., van Beek, R., Bierkens, M. F. P., Ligtvoet, W., and Winsemius, H. C.: Assessing flood risk at the global scale: model setup, results, and sensitivity, Environ. Res. Lett., 8, 044019, https://doi.org/10.1088/1748-9326/8/4/044019, 2013.
Wieland, M., Pittore, M., Parolai, S., Begaliev, U., Yasunov, P., Tyagunov, S., Moldobekov, B., Saidiy, S., Ilyasov, I., and Abakanov, T.: A Multiscale Exposure Model for Seismic Risk Assessment in Central Asia, Seismol. Res. Lett., 86, 210–222, https://doi.org/10.1785/0220140130, 2015.
Win, S., Zin, W. W., Kawasaki, A., and San, Z. M. L. T.: Establishment of flood damage function models: A case study in the Bago River Basin, Myanmar, Int. J. Disaster Risk Reduct., 28, 688–700, https://doi.org/10.1016/j.ijdrr.2018.01.030, 2018.
Wing, O. E. J., Pinter, N., Bates, P. D., and Kousky, C.: New insights into US flood vulnerability revealed from flood insurance big data, Nat. Commun., 11, 1444, https://doi.org/10.1038/s41467-020-15264-2, 2020.
World Bank, UNISDR, and CAREC: Central Asia and Caucasus Disaster Risk Management Initiative (CAC DRMI). Risk Assessment for Central Asia and Caucasus - Desk Study Review, 2012.
Yamazaki, Dai, et al. "A high-accuracy map of global terrain elevations." Geophysical Research Letters 44.11 (2017): 5844-5853.
Yamazaki, Dai, et al. "MERIT Hydro: A high-resolution global hydrography map based on latest topography dataset." Water Resources Research 55.6 (2019): 5053-5073.
Yu, Y., Pi, Y., Yu, X., Ta, Z., Sun, L., Disse, M., Zeng, F., Li, Y., Chen, X., and Yu, R.: Climate change, water resources and sustainable development in the arid and semi-arid lands of Central Asia in the past 30 years, J. Arid Land, 11, 1–14, https://doi.org/10.1007/s40333-018-0073-3, 2019.

Pagina 4: [1] ha eliminato	Gianbattista Bussi	26/04/24 15:47:00
Pagina 6: [2] ha eliminato	Gianbattista Bussi	29/04/24 09:31:00
Pagina 6: [2] ha eliminato	Gianbattista Bussi	29/04/24 09:31:00
Pagina 6: [2] ha eliminato	Gianbattista Bussi	29/04/24 09:31:00
Pagina 6: [3] ha eliminato	Gianbattista Bussi	29/04/24 09:32:00
Pagina 6: [3] ha eliminato	Gianbattista Bussi	29/04/24 09:32:00
Pagina 6: [4] ha eliminato	Gianbattista Bussi	29/04/24 09:32:00
Pagina 6: [4] ha eliminato	Gianbattista Bussi	29/04/24 09:32:00
Pagina 6: [5] ha eliminato	Gianbattista Bussi	29/04/24 09:32:00
Pagina 6: [5] ha eliminato	Gianbattista Bussi	29/04/24 09:32:00
Pagina 6: [6] ha eliminato	Gianbattista Bussi	29/04/24 09:32:00
Pagina 6: [6] ha eliminato	Gianbattista Bussi	29/04/24 09:32:00
Pagina 7: [7] ha eliminato	Simona Denaro	15/05/24 16:15:00
Pagina 7: [8] ha eliminato	Gianbattista Bussi	29/04/24 09:35:00
Pagina 7: [9] ha eliminato	Gianbattista Bussi	02/05/24 09:06:00
Pagina 16: [10] ha eliminato	Gianbattista Bussi	02/05/24 09:57:00
Pagina 17: [11] ha eliminato	Gianbattista Bussi	02/05/24 10:08:00
Pagina 17: [12] ha eliminato	Gianbattista Bussi	02/05/24 11:47:00
Pagina 19: [13] ha eliminato	Simona Denaro	15/05/24 21:52:00
Pagina 19: [14] ha eliminato	Denaro, Simona	15/05/24 22:07:00
Pagina 21: [15] ha eliminato	Gianbattista Bussi	13/05/24 10:49:00
Pagina 21: [16] ha eliminato	Gianbattista Bussi	13/05/24 10:49:00